

# RESSALVA

Atendendo solicitação do autor,  
o texto completo desta tese será  
disponibilizado somente a partir  
de 14/08/2021



UNIVERSIDADE ESTADUAL PAULISTA  
“JÚLIO DE MESQUITA FILHO”  
Câmpus de São José do Rio Preto

Jorge Enrique Hernández González

## **Computational Strategies for Selective Inhibition of Falcipain-2**

São José do Rio Preto  
2020

Jorge Enrique Hernández González

## **Computational Strategies for Selective Inhibition of Falcipain-2**

Tese apresentada como parte dos requisitos para obtenção do título de Doutor em Biofísica Molecular, junto ao Programa de Pós-Graduação em Biofísica Molecular, do Instituto de Biociências, Letras e Ciências Exatas da Universidade Estadual Paulista “Júlio de Mesquita Filho”, Câmpus de São José do Rio Preto.

Financiadora: FAPESP – Proc 2016/24587-9

CAPES

Orientador: Prof. Dr. Vitor Barbanti Pereira Leite

Coorientador: Prof. Dr. Pedro Geraldo Pascutti

São José do Rio Preto

2020

H557c	<p>Hernández-González, Jorge Enrique</p> <p>Computational strategies for selective inhibition of falcipain-2 / Jorge Enrique Hernández-González. -- São José do Rio Preto, 2020 186 f. : il., tabs.</p> <p>Tese (doutorado) – Universidade Estadual Paulista (UNESP), Instituto de Biociências, Letras e Ciências Exatas, São José do Rio Preto.</p> <p>Orientador: Vitor Barbanti Pereira Leite Coorientador: Pedro Geraldo Pascutti</p> <p>1. Biologia molecular. 2. Biofísica molecular. 3. Malária. 4. Plasmodium falciparum. 5. Dinâmica molecular. I. Título.</p>
-------	---

Sistema de geração automática de fichas catalográficas da Unesp. Biblioteca do Instituto de Biociências Letras e Ciências Exatas, São José do Rio Preto. Dados fornecidos pelo autor(a).

Essa ficha não pode ser modificada.

Jorge Enrique Hernández González

## **Computational Strategies for Selective Inhibition of Falcipain-2**

Tese apresentada como parte dos requisitos para obtenção do título de Doutor em Biofísica Molecular, junto ao Programa de Pós-Graduação em Biofísica Molecular, do Instituto de Biociências, Letras e Ciências Exatas da Universidade Estadual Paulista “Júlio de Mesquita Filho”, Câmpus de São José do Rio Preto.

Financiadora: FAPESP – Proc.. 2016/24587-9

CAPES – 031/2013 PRÓ-DEFESA 3

### Comissão Examinadora

Prof. Dr. Vitor Barbanti Pereira Leite  
UNESP – Câmpus de São José do Rio Preto  
Orientador

Prof. Dr. Sidney Jurado de Carvalho  
UNESP – Câmpus de São José do Rio Preto

Prof. Dr. Alexandre Suman de Araujo  
UNESP – Câmpus de São José do Rio Preto

Prof. Dr. Rodrigo Guerino Stabeli  
USP – Câmpus de Riberão Preto

Prof. Dr. Gustavo Troiano Feliciano  
UNESP – Câmpus de Araraquara

São José do Rio Preto

14 de fevereiro de 2020

*A aquellos que aun en medio de las  
adversidades mantienen viva la esperanza.*

## ACKNOWLEDGMENTS

I would like to thank God, our Lord. Without Him I would not be here today, without His love and mercy I would not have the strength and courage to move forward and face the obstacles of life.

I thank my daughter and my wife for their support, their company, their understanding and their true love. I am grateful to my mother for all the dedication and unconditional love she has given me throughout my life. My father, although not with us anymore, would be proud of his son's achievement. I am thankful for his support and guidance. Many thanks to my brother, my grandparents and the rest of the family. All of you dwell in a special place of my heart despite the distance.

I am very grateful to professor Pedro Pascutti for having trusted me when he barely knew me, and for having given me the opportunity to come to Brazil to pursue my career. I also thank professor Vitor Leite for having accepted me as his PhD student and for his constant support. Without both, this work would not have been possible.

Many thanks to my collaborators, especially Emir Salas, Pedro Valiente and Chris Oostenbrink for their contribution to this work. Thanks to my friends for making my life happier and worth living, and to my teachers, professors and former supervisors for having guided my first steps in Science. This study was financed in part by the Coordenação de Aperfeiçoamento de Pessoal de Nível Superior - Brasil (CAPES) - Finance Code 001: 031/2013 PRÓ-DEFESA 3.

I also thank FAPESP, for the concession of the research grant No. 2016/24587-9, Sao Paulo Research Foundation (FAPESP), which provided financial support to my PhD project during the last three years.

## RESUMO

A falcipaina-2 (FP-2) é uma hemoglobina-chave do *Plasmodium falciparum*, frequentemente selecionada como alvo para o planejamento de fármacos antimaláricos. Apesar dos esforços, nenhum inibidor da FP-2 tem entrado em fase de ensaios clínicos, pois a inibição cruzada de alvos humanos constitui um obstáculo. Neste trabalho, abordamos questões relacionadas à inibição seletiva da FP-2 através de diferentes técnicas computacionais, como simulações de dinâmica molecular, triagem virtual, ancoramento molecular, análise de comunidades e cálculos de volume de cavidades e energia livre. Ademais, realizamos ensaios de inibição *in vitro* para validar as predições. Apresentamos os compostos HTS07940 e HTS08262, que inibem a FP-2 e culturas de *P. falciparum* com boa seletividade respeito à catepsina K humana (hCatK) e à linha celular HeLa. Os inibidores foram identificados por meio de uma estratégia de triagem virtual que descartou ligantes com alta afinidade pela hCatK. Outras formas de atingir inibição seletiva são exploradas, como a busca por inibidores alostéricos, que ligam tipicamente sítios menos conservados. Analisamos uma região da FP-2 equivalente a um sítio alostérico da hCatK previamente caracterizado, o sítio 6, e predizemos vários ligantes potenciais. Após avaliação experimental, dois compostos, ZINC03225317 e ZINC72290660, são confirmados como inibidores não competitivos da FP-2, o que reforça a relevância deste sítio para o planejamento de fármacos. A busca de cavidades alostéricas é expandida a outros sítios, baseada em informações experimentais prévias relacionadas a uma *E*-chalcona identificada acidentalmente como inibidor não competitivo da FP-2. Os resultados revelam a ocorrência de uma cavidade transiente numa região denominada sítio 3, que permanece maioritariamente ocluída pela cadeia lateral do resíduo K34. O modo de ligação predito da *E*-chalcona é consistente com os dados experimentais disponíveis e fornece informação sobre o mecanismo alostérico a nível molecular. Por fim, estudamos os determinantes moleculares da alta seletividade pela FP-2 de nitrilos que contêm substituintes de 3-piridina em P2, previamente estudados. Segundo as nossas predições, pontes de água envolvendo os resíduos I85 e D234 da FP-2 e o nitrogênio da piridina explicam os perfis experimentais de atividade. Portanto, inibidores seletivos da FP-2 podem ser planejados promovendo a formação de pontes de água no fundo do subsítio S2 e/ou introduzindo grupos químicos que substituem a molécula de água envolvida.

**Palavras-chave:** Malária. *Plasmodium falciparum*. Falcipaina-2. Inibidores. Seletividade. Alostéria. Dinâmica molecular. Triagem virtual. Energia livre. Ensaios de inibição. Cavidades transientes. Modo de ligação. Comunidade. Rota de sinalização. Ponte de água.



## ABSTRACT

Falcpain-2 (FP-2) is a key hemoglobinase of *Plasmodium falciparum* that has been extensively targeted in antimalarial drug discovery projects. Despite the efforts, none of the existing FP-2 inhibitors has entered the clinical trials yet, as cross-inhibition of human off-targets remains a major concern. Here, we tackle issues related to selective FP-2 inhibition by employing different computational techniques, such as molecular dynamics simulations, virtual screening, docking, community analysis and pocket volume and free energy calculations. We also perform *in vitro* inhibition assays to validate the predictions. We report two compounds, HTS07940 and HTS08262, displaying inhibition against FP-2 and *P. falciparum* cultures with good selectivity with respect to human cathepsin K (hCatK) and HeLa cell line. The inhibitors were identified through a virtual screening strategy that ruled out ligands with high affinity for hCatK. Moreover, other ways to achieve selective inhibition are explored, such as the search for allosteric inhibitors, which bind to typically less conserved sites. We analyze an FP-2 region equivalent to a previously-characterized allosteric site of hCatK, termed site 6, and predicted various potential ligands. After experimental evaluation, two compounds, ZINC03225317 and ZINC72290660, are confirmed as non-competitive inhibitors of FP-2, thus reinforcing the suitability of site 6 as a druggable allosteric cavity. The search for potential cavities is expanded to other sites on the basis of previous experimental information related to a serendipitously-identified *E*-chalcone displaying non-competitive inhibition against FP-2. Our results reveal the occurrence of a transient pocket in a region termed site 3, which remains occluded most of the simulation time by the side-chain of residue K34. The predicted binding mode of the *E*-chalcone is consistent with the available experimental data and sheds light upon important features of the allosteric mechanism at molecular level. Finally, we study the molecular determinants of the high selectivity for FP-2 of previously-reported nitriles containing 3-pyridine substituents at P2. Our results reveal that water bridges involving residues I85 and D234 of FP-2, and the pyridine nitrogen, explain the experimental activity profiles. Therefore, selective FP-2 inhibitors can be designed by promoting the formation of water bridges at the bottom of the S2 subsite and/or by introducing substituents that replace the bridging water molecule.

**Keywords:** Malaria. *Plasmodium falciparum*. Falcpain-2. Inhibitors. Selectivity. Allostery. Molecular dynamics simulation. Virtual screening. Free energy. Inhibition assays. Transient pockets. Binding mode. Community. Signaling Pathway. Water bridge.

## FIGURE LIST

Figure 1.1. Life cycle of <i>P. falciparum</i> .....	17
Figure 1.2. Structural features of FP-2 and FP-3.....	19
Figure 1.3. Active sites of FP-2 and FP-3.....	20
Figure 1.4. Some examples of non-peptidic FP-2 inhibitors identified through SBVS directed towards the orthosteric site.....	22
Figure 1.5. Predicted and experimentally-confirmed allosteric sites in hCatK.....	23
Figure 1.6. Allosteric inhibitors of FP-2 reported in literature.....	24
Figure 1.7. FP-2 tryptic peptides displaying differences in their hydrolysis rates in the presence of either a competitive inhibitor or Cpd66.....	25
Figure 1.8. Chemical structures and experimental $IC_{50}$ values of the studied compounds against FPs and hCats.....	26
Figure 2.1. Workflow employed for the identification of allosteric inhibitors against FP-2.....	32
Figure 2.2. Schematic representation of a hypothetical potential energy function and several bias potentials.....	39
Figure 2.3. Thermodynamic cycles used to calculate $\Delta\Delta G$ values for the studied covalent complexes.....	44
Figure 3.1. Chemical structures, and identifier of the compounds selected from SBVSs.....	59
Figure 3.2. Dose-response curves for seven FP-2 inhibitors identified by SBVS.....	60
Figure 3.3. Structures of FP-2 in complex with compounds HTS07940 and HTS8262.....	63
Figure 3.4. Structural representation of the interfaces of compound HTS07940 bound to FP-3, hCatK and hCatK mutants.....	64
Figure 3.5. Mapping of hCatK site 6 onto the crystal structure of FP-2.....	68
Figure 3.6: Conformational variation of putative allosteric site 6 of FP-2 during GROMOS 54a8 MD simulations.....	69
Figure 3.7. Conformational variation of putative allosteric site 6 of FP-2 during Amber ff14SB MD simulations.....	70
Figure 3.8. Dose-response curves for the compounds displaying inhibitory activity against FP-2.....	72
Figure 3.9. Dose-response curves of the selected compounds obtained from the centrifuge counter-screen against FP-2.....	72
Figure 3.10. Determination of the inhibition mechanism of ZINC03225317 against FP-2.....	73
Figure 3.11. Determination of the inhibition mechanism of ZINC72290660 against FP-2.....	74
Figure 3.12. Predicted structures of FP-2 in complex with two non-competitive inhibitors.....	75
Figure 4.1. Formation of a transient pocket in the site 3 region of FP-2.....	81
Figure 4.2. Predicted binding mode of Cpd66 into the site 3 pocket of FP-2.....	83

Figure 4.3. Predicted structure of FP-2 in complex with a peptide and Cpd66.....	85
Figure 4.4. PMFs for the dissociation of Cpd66 from FP-2 in the absence and presence of the substrate.....	87
Figure 4.5. Community analysis for the studied systems.....	89
Figure 4.6. Communication pathways linking the allosteric and the active sites in four FP-2 systems.....	92
Figure 5.1. Distance time profiles and distributions during MD simulations of FP-2 in complex with 3Pyr- and 2Pyr-containing nitriles.....	101
Figure 5.2. Structural representation of the studied FP-2:nitrile complexes.....	102
Figure 5.3. Distance time profiles and distributions during MD simulations of FP-3 and hCats in complex with Nit3Pyr.....	106
Figure 5.4. Structural representation of Nit3Pyr in complex with FP-3 and various hCats.....	107
Figure A1. Workflow employed to parametrize the studied covalent inhibitors.....	134
Figure A2. Partial charges assigned to the atoms of the studied compounds.....	135
Figure A3. Atoms defining the TI regions during the alchemical transformations.....	136
Figure B1. Structural alignment of FPs and hCats, shown at the level of their primary sequences.....	145
Figure B2. MD simulations of two different protonation states of HTS07940 in complex with PfENR bound to NAD <sup>+</sup> .....	147
Figure B3. Selected docking poses of compound HTS07940 into the FP-2 binding site.....	148
Figure B4. Final conformations after 100 ns MD simulations of the docking poses of compound HTS07940 into the FP-2 binding site.....	149
Figure B5. Central structures obtained from clustering analysis of multiple aMD simulations of HTS07940 in complex with FP-2 and their respective $\Delta G_{eff}$ values.....	150
Figure B6. Central structures obtained from clustering analysis of multiple aMD simulations of HTS07940 in complex with FP-3 and their respective $\Delta G_{eff}$ values.....	151
Figure B7. Central structures obtained from clustering analysis of multiple aMD simulations of HTS07940 in complex with hCatK and their respective $\Delta G_{eff}$ values.....	152
Figure B8. Alternative ‘down’ conformation of Y67 in hCatK.....	153
Figure B9. Active sites of hCatK and FP-3.....	155
Figure B10. Distance distributions of residues Y67-L209 in free hCatK and in hCatK complex with HTS07940.....	156
Figure B11: Distance time profiles of interacting oppositely-charged residues of FP-2 site 6 during the simulations conducted with GROMOS 54a8 force-field.....	156
Figure B12: Distance time profiles of interacting oppositely-charged residues of FP-2 site 6 during the simulations conducted with Amber14SB force-field.....	157
Figure C1. Occlusion by residue K34 of site 3 internal cavity in FP-2 crystal structure 2OUL.....	158

Figure C2. Formation of a transient pocket in the site 3 region of FP-3.....	159
Figure C3. Best docking pose of Cpd66 into site 3.....	160
Figure C4. Time evolution of the FP-2:Cpd66 complex determined by docking during four independent MD simulations.....	161
Figure C5. Comparison of the docking and MD-generated conformations of Cpd66 in complex with FP-2.....	162
Figure C6. Contact between residue K203 and the six-membered aryl ring of Cpd66 in the FP-2:Cpd66 complex.....	162
Figure C7. Exchange of water molecules mediating the H-bond between Cpd66 and G29.....	163
Figure C8. RMSD time profiles for the Cpd66 and peptide during the replicate MD simulations of the studied complexes.....	164
Figure C9. Comparison of RMSD distributions and per-residue RMSF values for the studied systems.....	165
Figure C10. PCA results for the studied systems.....	167
Figure C11. Generalized correlations for the studied systems.....	168
Figure C12. Distribution of raw and filtered generalized correlations for the four studied systems.....	169
Figure C13. Dependency of modularity values on the number of communities for the analyzed systems...	170
Figure C14. Community analysis for the studied systems using a distance cut-off of 4.5 Å to define residue-residue contacts.....	170
Figure C15. Betweenness centralities for the FP-2 residues in four different states.....	172
Figure C16. Titration curves that were reliably estimated in only one system.....	173
Figure C17. Titration curves displaying the largest shifts upon Cpd66 binding to FP-2.....	174
Figure C18. Residues displaying significant $pK_a$ shifts upon the binding of Cpd66 to FP-2.....	175
Figure C19. RMSD values for the peptide at different pHs.....	175
Figure D1. Interaction of Nit3PyrH <sup>+</sup> , Nit2PyrH <sup>+</sup> and Nit4PyrH <sup>+</sup> with FP-2.....	177
Figure D2. Insertion of P2-Pyr moieties at different protonation states into the S2 subsite of FP-2.....	178
Figure D3. Distance distributions involving the water molecules closest to N <sub>pyr</sub> in three complexes.....	179
Figure D4. $\partial V/\partial \lambda$ vs $\lambda$ plots for the alchemical transformation of close and distant orientations in the hCatL:Nit3Pyr complex.....	180
Figure D5. $\partial V/\partial \lambda$ vs $\lambda$ plots for all the alchemical transformation conducted during the $\Delta\Delta G$ calculations.....	183
Figure D6. Distance distributions and central structures of free FP-2 and FP-3 corresponding to every distribution peak.....	185

## TABLE LIST

Table 3.1. Autodock-Vina scores for the selected compounds.....	58
Table 3.2. $IC_{50}$ values and selectivity indices for the selected compounds.....	61
Table 3.3 MM-GBSA free energy values for the studied complexes.....	67
Table 3.4. Compounds selected after refinement of SBVSs against different conformations of FP-2 site 6.....	71
Table 3.5. $K_i$ and alpha values for the noncompetitive inhibitors of FP-2.....	75
Table 4.1: MM-GBSA free energy values for the studied complexes.....	86
Table 4.2: Results of the $\Delta G^{\circ}_{bind}$ calculations through US for the interaction of Cpd66 with free FP-2 and the FP-2:peptide complex.....	88
Table 5.1. Fractional occupancies of water bridges and H-bonds involving the P2-Pyr moiety of the studied nitriles in complex with FP-2.....	104
Table 5.2. Fractional occupancies of water bridges and H-bonds involving the $N_{pyr}$ atom of Nit3Pyr in complex with FP-3 and various hCats.....	109
Table 5.3: $\Delta\Delta G$ values for several nitriles bound to FP-2 with respect to the FP-2:Nit3Pyr complex.....	110
Table 5.4. Energy contribution of water bridges of Nit3Pyr in complex with FPs and hCats calculated through MM-GBSA.....	114
Table B1: %IDs for hCats with respect to FP-2 and FP-3 in the active site region.....	146
Table B2. $\Delta G_{eff}$ -values for the last 3 ns of the MD simulations of the docking poses of compound HTS07940 in complex with FP-2.....	150
Table B3. Free energy values for the two top-scoring poses of HTS07940 in complex with hCatK during a 100 ns MD simulation.....	154
Table C1. Residue composition of each community of the studied systems using a 5.0 Å distance cut-off for residue-residue contact definition.....	169
Table C2. Residue composition of each community of the studied systems using a 4.5 Å distance cut-off for residue-residue contact definition.....	171
Table D1: Relative free energies between FP-2:Nit3PyrH <sup>+</sup> and FP-2:Nit3Pyr complexes.....	178
Table D2: Relative free energies between the distant and close orientations of Nit3Pyr in complex with hCatL.....	181
Table D3. Fractional occupancies of water bridges and H-bonds involving I85 and D234 of free FP-2 and FP-2:Nit3Pyr, and I87 and E236 of FP-3 and FP-3:Nit3Pyr.....	186

## ABBREVIATIONS AND SYMBOLS

<b>2D</b>	Two-dimensional
<b>3D</b>	Three-dimensional
<b>AMC</b>	7-amino-4-methyl coumarin
<b>aMD</b>	Accelerated Molecular Dynamics
<b>APBS</b>	Adaptive Poisson-Boltzmann Solver
<b>CA</b>	Community Analysis
<b>CC<sub>50</sub></b>	Half-Maximal Cytotoxic Concentration
<b>Cpd48</b>	Compound 48
<b>Cpd66</b>	Compound 66
<b>CpHMD</b>	Constant pH Molecular Dynamics
<b>CQ</b>	Chloroquine
<b>DDT</b>	Dithiothreitol
<b>DMEM</b>	Modified Eagle's Medium
<b>DMSO</b>	Dimethyl sulfoxide
<b>E64</b>	<i>trans</i> -epoxysuccinyl-L-leucylamido(4-guanidino)butane
<b>EM</b>	Energy Minimization
<b>ENR</b>	Enoyl Reductase
<b>ESP</b>	Electrostatic Potential
<b>FBS</b>	Fetal Bovine Serum
<i>f<sub>d</sub></i>	Fraction of Deprotonation
<b>FEP</b>	Free Energy Perturbation
<b>ff14SB</b>	ff14SB Amber Force-Field
<b>FP-2</b>	Falcipain-2
<b>FP-3</b>	Falcipain-3
<b>FPs</b>	Falcipains
<b>gaff</b>	Generalized Amber Force-Field
<b>GC</b>	Generalized Correlation
<b>H-Bond</b>	Hydrogen Bond
<b>hCatB</b>	Human Cathepsin B
<b>hCatK</b>	Human Cathepsin K

<b>hCatL</b>	Human Cathepsin L
<b>hCatS</b>	Human Cathepsin S
<b>hCats</b>	Human Cathepsins
<b>HEPES</b>	4-(2-hydroxyethyl)-1-piperazineethanesulfonic acid
<b>IC<sub>50</sub></b>	Half-Maximal Inhibitory Concentration
<b>ID</b>	Sequence Identity
<b>InhA</b>	Enoyl Reductase of <i>Mycobacterium tuberculosis</i>
<b>K<sub>a</sub></b>	Acid Dissociation Constant
<b>K<sub>i</sub></b>	Inhibition Constant
<b>K<sub>M</sub></b>	Michaelis-Menten Constant
<b>K<sub>s</sub></b>	Dissociation Constant of the Enzyme-Substrate complex
<b>LINCS</b>	Linear Constraint Solver
<b>MD</b>	Molecular Dynamics
<b>MM-GBSA</b>	Molecular Mechanics Poisson-Boltzmann Surface Area
<b>NADH</b>	Reduced Nicotinamide Adenine Dinucleotide
<b>Nit</b> bonded.	Core structure of nitriles shown in Fig. 1.5, to which the variable P2 substituent (X) is bonded.
<b>NPT</b>	Isothermal-Isobaric Ensemble
<b>N<sub>pyr</sub></b>	Pyridine nitrogen
<b>NVT</b>	Isothermal-Isochoric Ensemble
<b>PBS</b>	Phosphate-Buffered Saline
<b>PC</b>	Principal Component
<b>PCA</b>	Principal Component Analysis
<b>PDB</b>	Protein Data Bank
<b>PfENR</b>	<i>Plasmodium falciparum</i> Enoyl Reductase
<b>PME</b>	Particle Mesh Ewald
<b>PMF</b>	Potential of Mean Force
<b>POVME</b>	Pocket Volume Measurer
<b>Pyr</b>	Pyridine
<b>RESP</b>	Restrained Electrostatic Potential
<b>RMSD</b>	Root Mean Square Deviation
<b>RMSF</b>	Root Mean Square Fluctuation

<b>RPMI</b>	Roswell Park Memorial Institute
<b>SASA</b>	Solvent Accessible Surface Area
<b>SBVS</b>	Structure-Based Virtual Screening
<b>SEM</b>	Standard Error of the Mean
<i>S<sub>vina</sub></i>	Autodock-Vina Energy Score.
<b>TI</b>	Thermodynamic Integration
<b>US</b>	Umbrella Sampling
<b>WHO</b>	World Health Organization
<b>WISP</b>	Weighted Implementation of Suboptimal Paths
<b><math>\alpha</math></b>	Ratio of the dissociation constant between the enzyme:inhibitor complex and the substrate to that of the free enzyme and the substrate
<b><math>\Delta G</math></b>	Gibbs Free Energy
<b><math>\Delta G^{\bullet}_{bind}</math></b>	Absolute Binding Free Energy with correction of the standard state.
<b><math>\Delta G_{bind}</math></b>	Binding Free Energy calculated through MM-GBSA
<b><math>\Delta G_{eff}</math></b>	Effective Free Energy
<b><math>\Delta G_R</math></b>	Free Energy of releasing the <i>xy</i> orthogonal restraints in the bound state
<b><math>\Delta S_{conf}</math></b>	Configurational Entropy
<b><math>\Delta\Delta G</math></b>	Relative Free Energy



## Table of Contents

<b>1 INTRODUCTION</b> .....	17
<b>2 MATERIAL AND METHODS</b> .....	29
<b>2.1 Computational section</b> .....	29
2.1.1 Preparation of the protein structures .....	29
2.1.2 Structure-based virtual screenings and rescoring steps .....	29
2.1.3 Prediction of the structures of FP-2 in complex with Cpd66 and the studied nitriles .....	32
2.1.4 Compound parametrization for MD simulations.....	33
2.1.5 Conventional MD Simulations.....	33
2.1.6 Accelerated MD simulations .....	37
2.1.7 Constant pH MD simulations .....	39
2.1.8 MM-GBSA free energy calculations.....	40
2.1.9 Thermodynamic integration free energy calculations .....	43
2.1.10 Umbrella sampling free energy calculations .....	45
2.1.11 Pocket volume measurements .....	48
2.1.12 Community analysis and calculation of optimal and suboptimal paths .....	48
2.1.13 Principal Component Analysis .....	50
2.1.14 Miscellaneous trajectory analyses .....	51
<b>2.2 Experimental section</b> .....	52
2.2.1 Expression and purification of recombinant enzymes.....	52
2.2.2 <i>In vitro</i> enzymatic assays of compounds selected from SBVSs targeting the active site.....	53
2.2.3 <i>In vitro</i> antiplasmodial activity assay .....	53
2.2.4 Cytotoxicity assays.....	54
2.2.5 Compounds from ZINC12 database.....	54
2.2.6 Activity assays of potential allosteric inhibitors against FP-2 .....	55
2.2.7 Centrifuge counter-screening .....	56
2.2.8 Determining mode of inhibition and $K_i$ value of active compounds .....	56
<b>3 IDENTIFICATION OF FALCIPAIN-2 INHIBITORS THROUGH AN INTEGRATED <i>IN SILICO</i> AND EXPERIMENTAL APPROACH</b> .....	58
<b>3.1 Identification of FP-2 inhibitors targeting the enzyme active site</b> .....	58
3.1.1 <i>In silico</i> identification of selective FP-2 inhibitors from Maybridge HitFinder™ Database .....	58
3.1.2 Experimental evaluation of the selected compounds .....	59
3.1.3 Prediction of the binding modes of HTS08262 and HTS07940 to FP-2.....	62

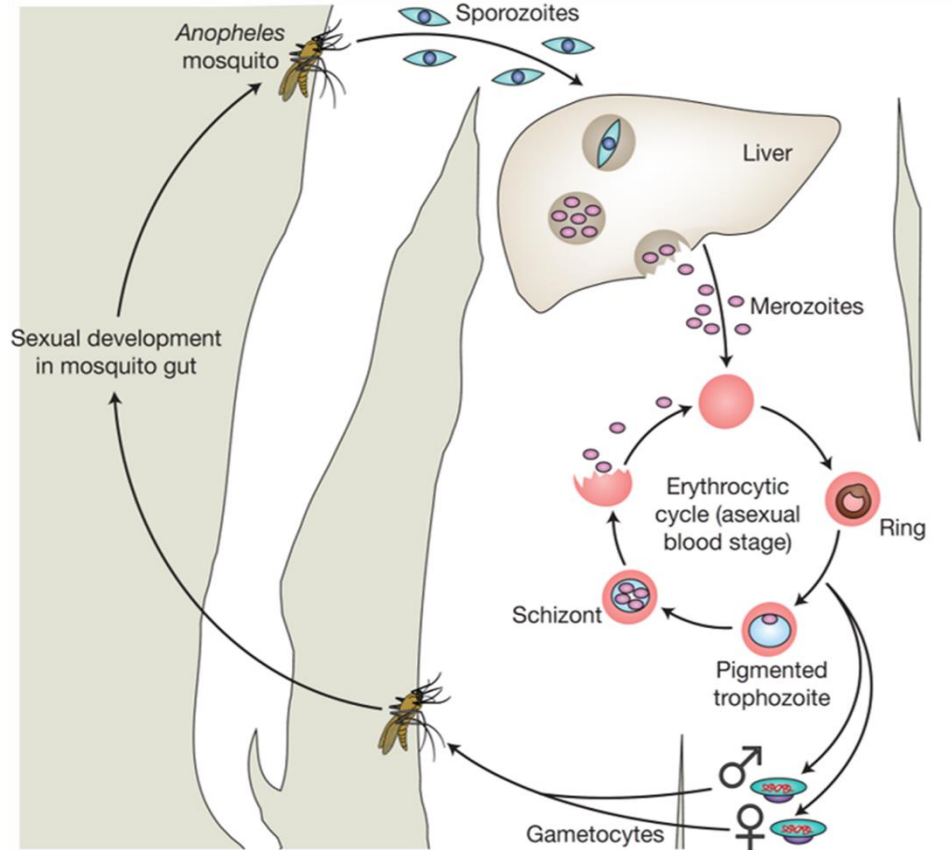
3.1.4 Prediction of the binding modes of HTS07940 to FP-3 and to hCatK.....	63
3.1.5 Calculation of the MM-GBSA free energies for the studied complexes.....	66
<b>3.2 Identification of non-competitive FP-2 inhibitors</b> .....	<b>68</b>
3.2.1 <i>In silico</i> identification of potential allosteric inhibitors of FP-2 targeting site 6.....	68
3.2.2 Experimental characterization of the potential allosteric inhibitors of FP-2.....	69
3.2.3 Structures of FP-2 in complex with the active non-competitive inhibitors .....	74
<b>3.3 Discussion</b> .....	<b>76</b>
<b>4 PROBING A NOVEL ALLOSTERIC SITE OF FALCIPAIN-2 THROUGH THE PREDICTION OF A NON-COMPETITIVE INHIBITOR BINDING MODE</b> .....	<b>80</b>
<b>4.1 Structural analyses</b> .....	<b>80</b>
4.1.1 Formation of a transient pocket at the site 3 region of FP-2 .....	80
4.1.2 Prediction of Cpd66 binding mode .....	82
<b>4.2 Energetic analyses</b> .....	<b>84</b>
4.2.1 Impact of Cpd66 binding on the affinity of FP-2 for the substrate .....	84
4.2.2 Calculation of standard binding free energies for FP-2 and Cpd66 in the presence and absence of the peptide.....	87
<b>4.3 Community, pathway and <math>pK_a</math> analyses</b> .....	<b>88</b>
4.3.1 Analysis of community rearrangements in the studied systems.....	88
4.3.2 Perturbations of signal propagation patterns across the FP-2 structure caused by Cpd66.....	91
4.3.3 $pK_a$ shifts in various FP-2 ionizable residues upon Cpd66 binding .....	94
<b>4.4 Discussion</b> .....	<b>96</b>
<b>5 ROLE OF WATER BRIDGES IN THE AFFINITY AND SELECTIVITY FOR FP-2 OF NITRILES BEARING PYRIDINE SUBSTITUENTS AT P2</b> .....	<b>100</b>
<b>5.1 Structural analyses</b> .....	<b>100</b>
5.1.1 Analysis of H-bonds and water bridges between P2-Pyr substituents and FP-2 residues.....	100
5.1.2 Analysis of H-bonds and water bridges between the 3Pyr substituent and S2 residues of FP-3 and hCats .....	105
<b>5.2 Energetic analyses</b> .....	<b>109</b>
5.2.1 Prediction of relative affinities of the studied nitriles for FP-2.....	109
5.2.2 Energy contributions of water bridges to the affinity of Nit3Pyr for the studied enzymes.....	113
<b>5.3 Discussion</b> .....	<b>116</b>
<b>6 CONCLUDING REMARKS</b> .....	<b>119</b>
<b>REFERENCES</b> .....	<b>121</b>
<b>APPENDIX A – Additional information to methods</b> .....	<b>134</b>

<b>APPENDIX B – Additional information to identification of FP-2 inhibitors through an integrated <i>in silico</i> and experimental approach .....</b>	<b>145</b>
<b>APPENDIX C – Additional information to the prediction of the binding mode of compound 66 to FP-2 and to the molecular mechanism of the exerted non-competitive inhibition .....</b>	<b>158</b>
<b>APPENDIX D – Additional information to the role of water bridges in the affinity and selectivity for FP-2 of nitriles bearing pyridine substituents at P2.....</b>	<b>176</b>

## 1 INTRODUCTION

Malaria is still a major problem of public health. Nearly half of the world's population lives in areas where this disease is endemic, mainly in tropical low-income countries.<sup>1,2</sup> According to the World Health Organization (WHO), approximately 290 million cases and 435 000 related deaths were reported in 2017.<sup>2</sup> The disease is caused in humans by five species of Plasmodia, i.e., *P. falciparum*, *P. ovale*, *P. vivax*, *P. malariae* and *P. knowlesi*, the former being responsible for the most lethal form of the disease.<sup>3,4</sup> Unfortunately, after a period of success in controlling malaria worldwide, the progress has stalled over the last years.<sup>2</sup>

**Figure 1.1. Life cycle of *P. falciparum*.** The parasites have a complex life cycle involving female mosquitoes of the genus *Anopheles*, where they undergo a sexual development, and human beings, where the asexual blood stage inside the erythrocytes takes place.



Source: Taken from ref. 5.

The life cycle of malaria parasites is complex and involves a number of different asexual and sexual developmental stages within both the vector and the vertebrate host (Fig. 1.1). In humans the disease is transmitted when bitten by an infected female *Anopheles* mosquito. The sporozoites are then injected into the dermal tissue and actively move into the circulatory system

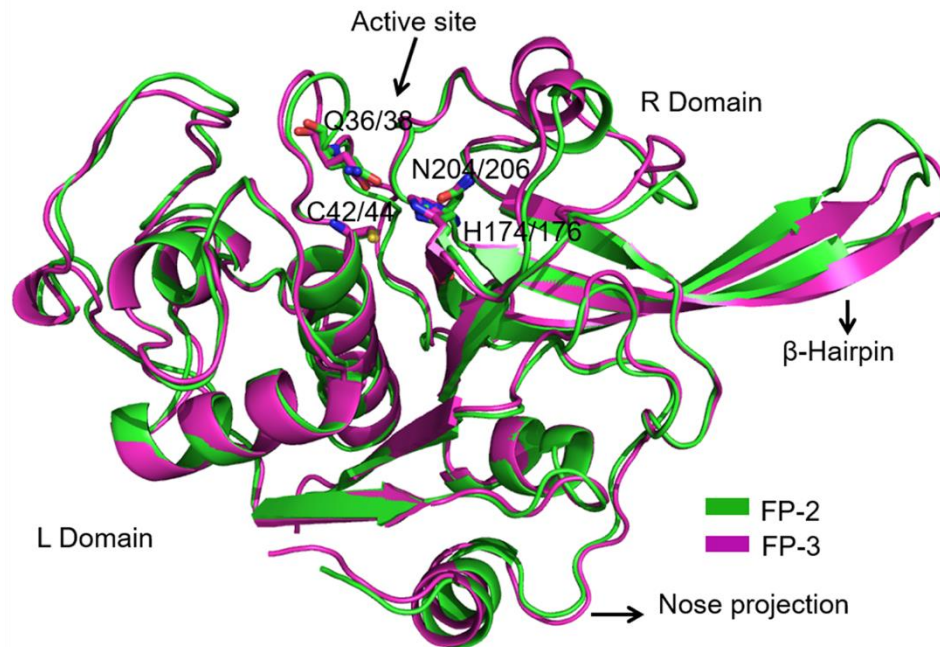
and colonize the liver.<sup>3</sup> Once in the liver, each sporozoite differentiates and divides into thousands of merozoite forms, which are released from hepatocytes into the bloodstream and invade the circulating erythrocytes. Within the new host cell, the parasite undergoes a maturation process from a ring-stage trophozoite to a pigmented trophozoite before finally undergoing mitotic nuclear divisions into daughter merozoites at the schizont stage. At this point, the infected erythrocytes rupture and release daughter merozoites into the bloodstream, which resume another round of asexual reproduction after having infected new erythrocytes.<sup>3</sup> Finally, some parasites differentiate into sexual forms, called gametocytes, which may be ingested by a feeding mosquito and undergo a sexual life cycle within the vector leading to parasite transmission to other human beings.<sup>3</sup>

The efforts to control malaria have been focused on two main approaches, i.e., killing the vector and killing the parasite. The first alternative comprises the extensive use of insecticides and habitat transformations, i.e., use of bed nets. Although this would be the most desirable method, its implementation has been largely unsuccessful due to the vast areas involved and the emergence of insecticide-resistant mosquito strains.<sup>3</sup> Alternatively, human beings can be immunized against malaria parasites. However, none of the developing vaccines is functional yet and there are no prospects for any of them to become available soon. In fact, the most promising vaccine to date, termed RTS,S, has shown, upon completion of phase III clinical trial, that its efficacy is limited and its effect depends on the geographic region.<sup>6</sup> Therefore, drug therapy remains an important approach to treat and prevent this infectious disease.<sup>3,7</sup>

The discovery of antimalarials has been mostly serendipitous and the mechanism of action is still largely unknown for many of them.<sup>3</sup> Most drugs are directed against blood-stage parasites. Chloroquine and other quinine alkaloids derivatives were extensively used to treat malaria during the 20<sup>th</sup> century across the world. Antifolate drugs, such as pyrimethamine, an inhibitor of folate metabolism, constitute another group of antimalarials. New drugs based on the artemisinin scaffold have been discovered during the last decades.<sup>3</sup> Currently, however, the emergence of *P. falciparum* strains resistant to the available drugs is becoming a great concern, as it poses a tremendous challenge for disease control in most parts of the world. Therefore, the development of new antimalarials is urgently needed, as well as the concomitant search for new drug targets.<sup>7</sup> Regarding the latter aspect, a great progress has been made since the unveiling of *P. falciparum* genome in 2002.<sup>3</sup> Potential drug targets have been grouped into three main categories, based on their function during the parasite's life cycle: *i*) targets involved in macromolecular and metabolite synthesis, *ii*)

targets associated with membrane transport and signaling and *iii*) targets involved in hemoglobin degradation.<sup>3</sup> Of note, process (*iii*) occurs within the food vacuoles of intraerythrocytic malaria parasites, and is carried out by a variety of proteases acting at an optimum pH within the range of 4.5-5.0, i.e., that of the food vacuole.<sup>8</sup> Amino acids derived from hemoglobin degradation are incorporated into parasite proteins or utilized as an energy source. It has also been suggested that removal of hemoglobin during its breakdown provides space in the erythrocyte for parasite growth and prevents early erythrocyte lysis.<sup>8</sup>

**Figure 1.2. Structural features of FP-2 and FP-3.** Both enzymes have the typical folding of C1 cysteine proteases, which consists of two domains. Mature FP-2 and FP-3 are made up of single polypeptides of 241 and 243 residues, respectively and share a 68% of sequence identity (ID).<sup>4, 8</sup> The catalytic residues of FP-2/3 are shown as sticks and labeled accordingly. The distinctive  $\beta$ -hairpin and nose-like insertions of both FPs are indicated by arrows. The crystal structures of FP-2 and FP-3 2OUL and 3BWK were taken for representation.

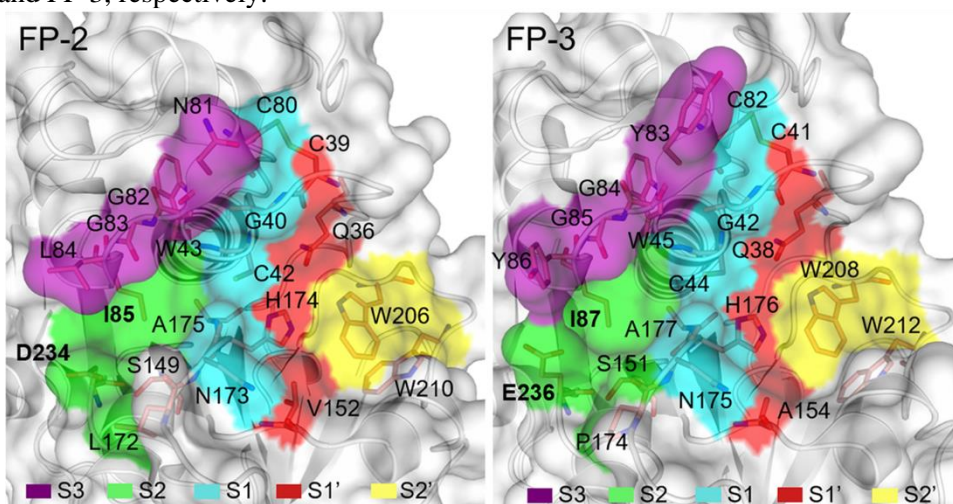


Source: Prepared by the author.

The abrogation of hemoglobin degradation with a variety of protease inhibitors leads to parasite death, thereby indicating the importance of hemoglobin-degrading enzymes as antimalarial drug targets. Among them, the *P. falciparum* C1 cysteine proteases, termed falcipain-2 (FP-2)<sup>9</sup> and falcipain-3 (FP-3)<sup>10</sup>, are considered as particularly promising targets for antimalarial drug discovery.<sup>4, 7, 8, 11</sup> Both proteases are synthesized as membrane-bound proforms that are processed to soluble mature forms probably by auto-proteolysis after exiting the endoplasmic reticulum/Golgi network. Besides being associated with hemoglobinase activity, FP-2 and FP-3 are involved in the

conversion of proplasmepsins, another group of hemoglobin-degrading aspartic proteases, into their mature active forms. FP-2 is also engaged in the degradation of erythrocyte membrane skeletal proteins at neutral pH, which suggests its involvement in erythrocyte rupture and release of mature merozoites into the bloodstream.<sup>8</sup> The disruption of FP-2 gene leads to trophozoites with swollen, dark-staining food vacuoles, consistent with markedly diminished hemoglobin degradation. However, more mature knockout parasites display normal phenotypes. In contrast to these results, repeated attempts to obtain FP-3 knockout parasites have been unsuccessful, although replacement of the FP-3 gene with a functional copy encoding a tagged protease was readily accomplished.<sup>4, 8, 12</sup> This indicates that FP-3 is essential to intraerythrocytic parasites and, thus, the development of cysteine protease inhibitors as antimalarial drugs should be directed against both FP-2 and FP-3.<sup>8</sup>

**Figure 1.3. Active sites of FP-2 and FP-3.** The active sites of both enzymes are made up of five subsites, from S3 to S2', which are colored differently according to the legend. The most important residues are shown as sticks and labeled accordingly. The representations correspond to the crystal structures 2OUL and 3BWK of FP-2 and FP-3, respectively.



Source: Prepared by the author.

According to the information provided by the available crystal structures, FP-2 and FP-3 adopt the classical papain-like fold, which is divided into L (left) and R (right) domains and the active site is located in a cleft at the junction between them (Fig 1.2). Four conserved catalytic residues, i.e., Q36/38, C42/44, H174/176 and N204/206, are present in the active sites of FP-2/FP-3, respectively (Fig. 1.2).<sup>13</sup> In spite of the common features shared by both FPs with the other papain-like proteases, they possess some unusual structural characteristics, such as an ‘arm-like’  $\beta$ -hairpin (near the C-terminus), which extends away from the protein surface, and a ‘nose-like’ projection (at the N terminus) (Fig.1.2). The arm-like structure may act as a distal site for

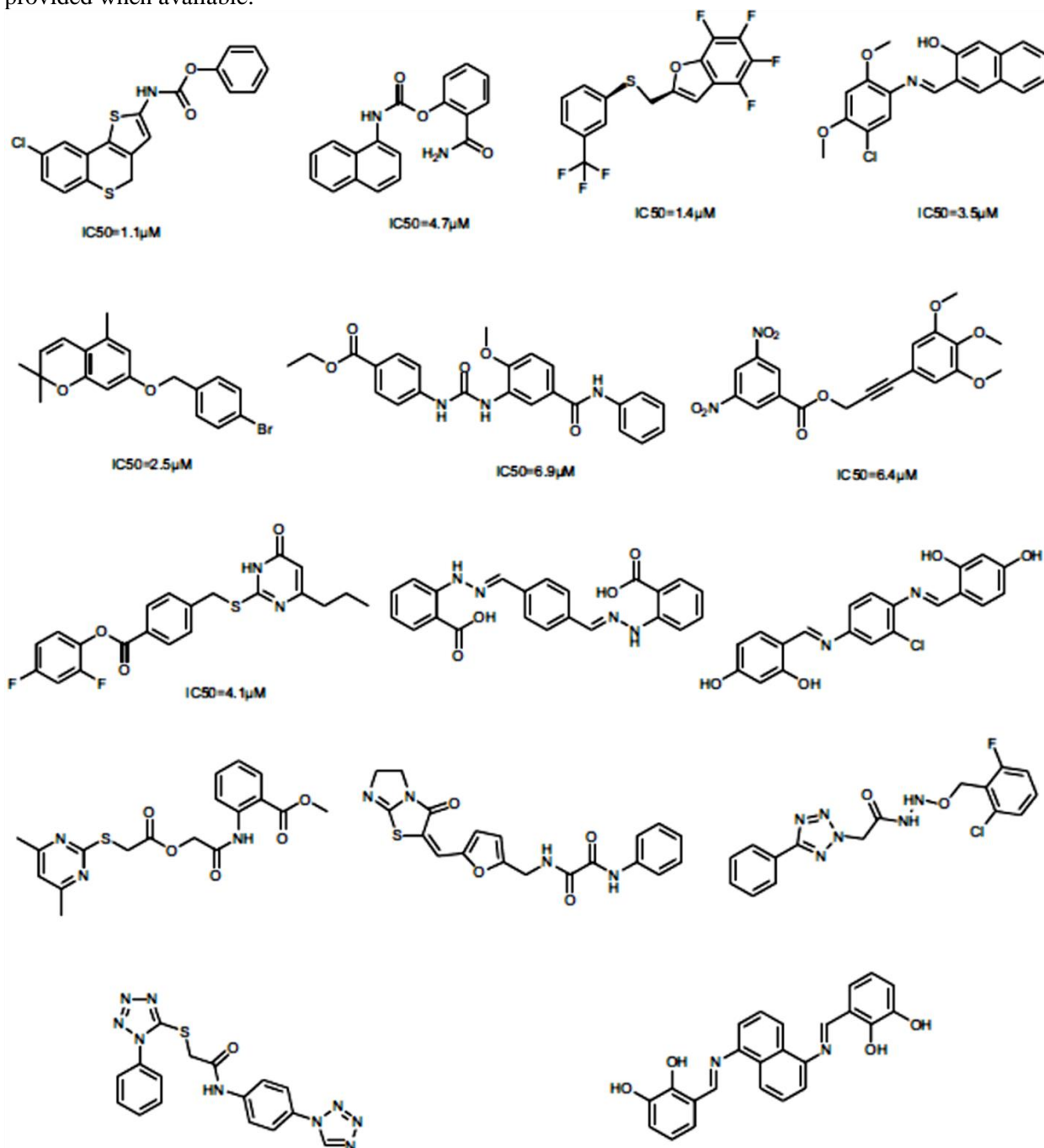
hemoglobin binding, as suggested by mutagenesis studies carried out with FP-2.<sup>14</sup> It also displays a great flexibility due to solvent exposure as shown by the analysis of different FP-2 crystal structures.<sup>8</sup> On the other hand, the nose-like projection is essential to proper folding according to deletion analysis of its sequence in FP-2.<sup>15</sup> Because of the great structural similarity of FP-2 and FP-3, it is likely for the nose-like projection to play an analogous role in the latter.

The active sites of FPs are formed by five subsites: S3, S2, S1, S1' and S2' (Fig. 1.3). The substrate-specificity requirements of the different subsites of FP-2 and FP-3 have been already studied and, despite the sequence similarity of both FPs, some differences in substrate specificity were observed.<sup>16</sup> The S1 subsite of FP-2 preferentially accommodates Arg residues at the P1 site, while that of FP-3 prefers Leu. The S2 subsites of both FPs have strict preference for Leu at P2. The S3 subsite of FP2 is rather promiscuous, while Ala at P3 is preferred by the S3 subsite of FP-3. The S1' subsite of FP-2 preferentially accommodates hydrophobic residues at P1' and that of FP-3 shows specificity for Arg residues at this site. The specificity of a fifth subsite, S2', was also assessed but it demonstrated no clear preference for any particular residue. These results can contribute to devise drug design strategies targeting both FPs.<sup>16</sup>

Over the past two decades, dozens of works have reported the discovery of FP-2 (and FP-3) inhibitors, some of them active against *P. falciparum* cultures.<sup>7, 8, 11, 17</sup> However, none of the existing candidates has entered clinical trials yet, and the search for novel inhibitors continues.<sup>7</sup> In general, the FP inhibitors can be grouped in three main categories according to their chemical structures: *i*) peptide-based, *ii*) peptidomimetics and *iii*) non-peptidic inhibitors.<sup>4, 7, 8, 11</sup> Remarkably, peptide-based inhibitors may display high affinities for FPs, as well as the capacity to inhibit the growth of malaria parasite cultures at sub-micromolar and even at nanomolar concentrations.<sup>7, 8</sup> In addition some of them have shown antimalarial effects *in vivo* using *P. vickei*-infected mice.<sup>4</sup> Despite the previous achievements, the use of peptide-based inhibitors in therapy is limited due to their susceptibility to protease degradation, low capacity to penetrate biological membranes and immunogenicity.<sup>8, 18</sup> Therefore, in an attempt to overcome the above drawbacks of peptide-based inhibitors, the search for other inhibitor classes, e.g., peptidomimetic and nonpeptidic compounds, has been conducted.<sup>7, 8, 11</sup> In this sense, structured-based virtual screening (SBVS) of compound databases has been successfully employed to identify many FP-2 inhibitors, especially of non-peptidic nature (Fig. 1.4).<sup>7</sup> This underscores the potential of computational approaches to discover new antimalarials.



**Figure 1.4.** Some examples of non-peptidic FP-2 inhibitors identified through SBVS directed towards the orthosteric site. The half maximal concentration ( $IC_{50}$ ) values against the enzyme are provided when available.

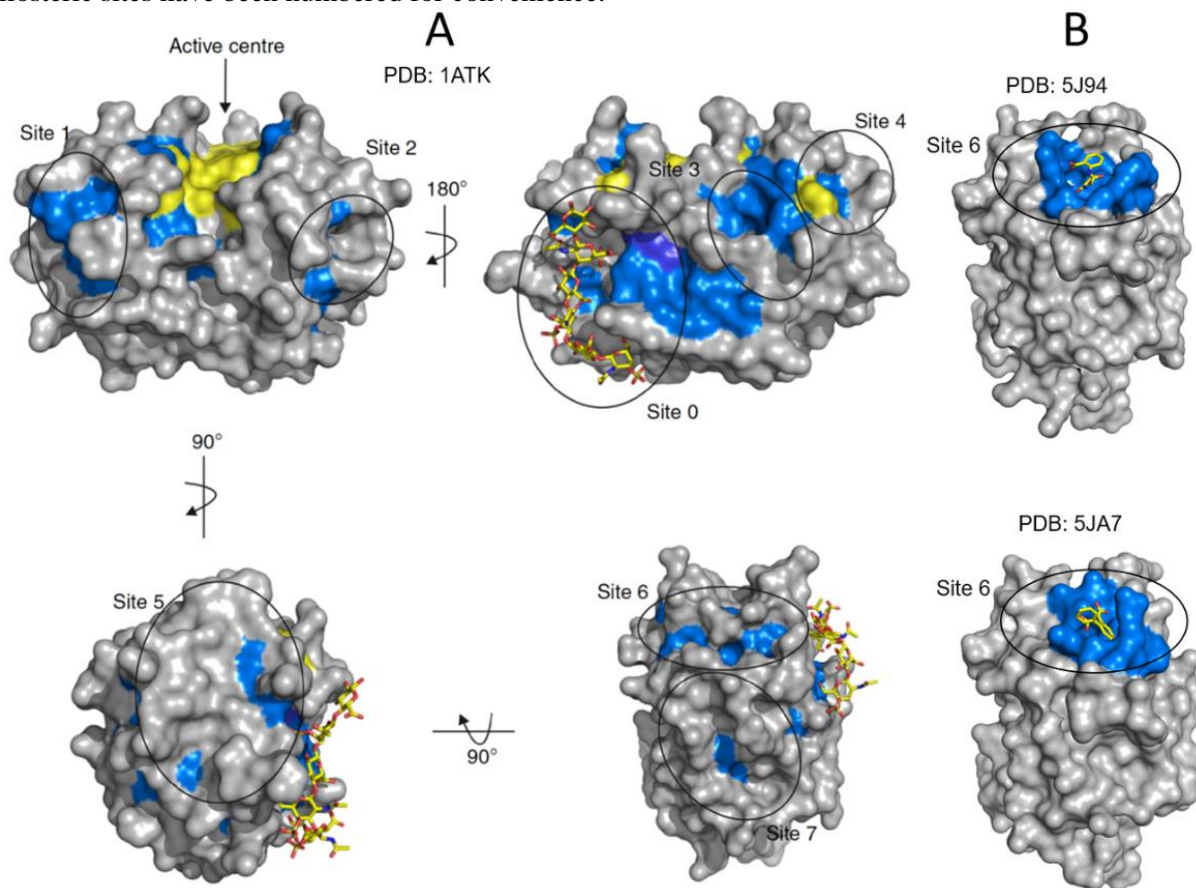


Source: Taken from ref. 7.

One of the main concerns regarding the identification of drugs against cysteine proteases is the likely occurrence of off-target effects due to lack of selectivity.<sup>19</sup> A promising way to tackle selectivity issues of molecules binding the orthosteric sites, i.e., the primary functional sites, of

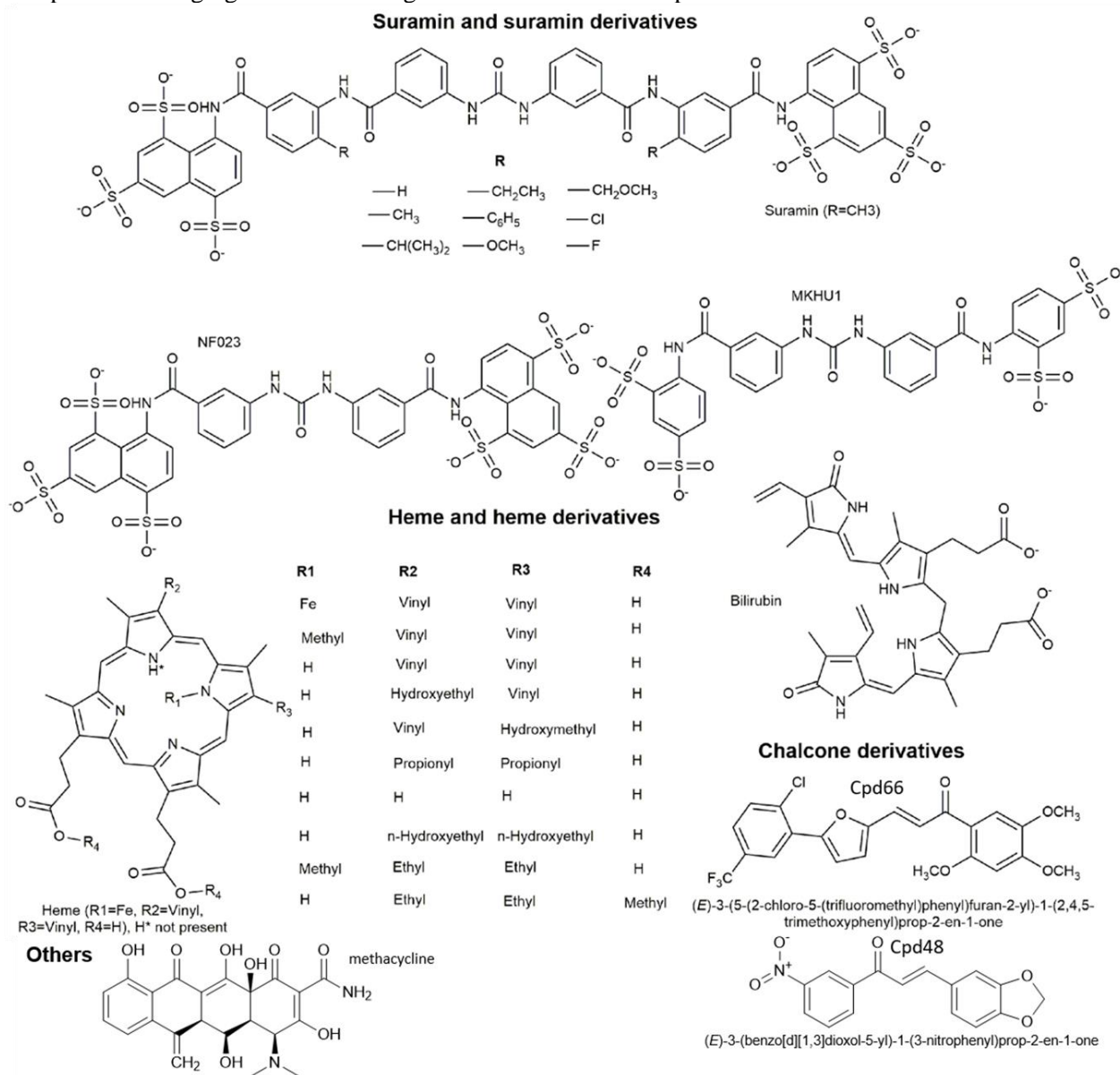
target proteins is the search for allosteric inhibitors, i.e., molecules that reduce the functional activity by binding to regions different from the orthosteric site.<sup>20-23</sup> In fact, allosteric inhibitors typically bind to protein regions that are less subjected to evolutionary pressure; which, in turn, increases the sequence divergence in the allosteric sites of proteins of the same family if compared to that of the orthosteric sites.<sup>23</sup> Interestingly, allostery has been already reported for various papain-like proteases, such as human cathepsins K, B and S (hCatK, hCatB and hCatS, respectively), cathepsin L-like proteases of *Leishmania mexicana*, *Trypanosoma cruzi* and *Trypanosoma brucei*, papain and FP-2 itself.<sup>24-38</sup> Therefore, the search for allosteric inhibitors against these proteases is supported by abundant experimental findings.

**Figure 1.5. Predicted and experimentally-confirmed allosteric sites in hCatK.** **A)** Allosteric sites on the surface of hCatK predicted through statistical coupling analysis. Sector and well-conserved residues are depicted in blue and yellow, respectively, the remaining residues are shown in gray. The structure of chondroitin sulfate, an already-known allosteric modulator of hCatK (PDB: 3C9E) was superimposed on the protein structure. **B)** Representation of the crystal structures of the allosteric inhibitors NSC13345 (up) and NSC94914 (down). Note that both inhibitors are bound to site6 of hCatK (residues depicted in blue). Allosteric sites have been numbered for convenience.



Source: Fig. 1.5-A adopted from ref. 25 and Fig. 1.5-B prepared by the author.

**Figure 1.6. Allosteric inhibitors of FP-2 reported in literature.** The reported inhibitors can be grouped in four main scaffolds shown in the figure. Suramin and heme trigger an excess-substrate inhibition. The compounds belonging to the remaining scaffolds act as noncompetitive inhibitors.

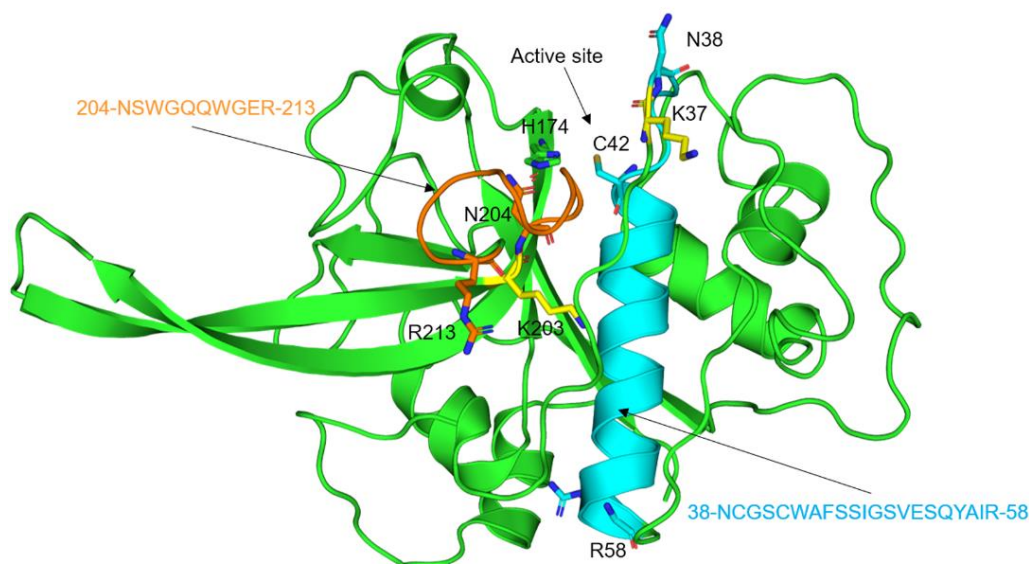


Source: Prepared by the author.

Remarkably, a previous work has proposed potential allosteric cavities in hCatK by analyzing co-evolving residues in multiple sequence alignment of the C1 cysteine proteases (Fig. 1.5-A).<sup>25</sup> The authors then reported several non-competitive inhibitors of hCatK discovered through SBVS directed against the promising cavities, including two with available co-crystal structures targeting the so-called site 6 (Fig. 1.5-B).<sup>25-27</sup> This information is relevant for the

identification of other allosteric inhibitors against cysteine proteases by means of structure-based computational approaches.

**Figure 1.7. FP-2 tryptic peptides displaying differences in their hydrolysis rates in the presence of either a competitive or a noncompetitive inhibitor.** The tryptic peptide shown in blue is protected from trypsin degradation in the presence of an orthosteric ligand, whereas the one depicted in orange becomes protected when the noncompetitive inhibitor Cpd66 binds the enzyme.<sup>36</sup> Trypsin cleavage sites are highlighted by depicting the residues forming the scissible peptide bond as sticks. In addition, the residues of the catalytic diad, C42 and H174, are represented as sticks. The primary sequences of the tryptic peptides are also included in the figure.

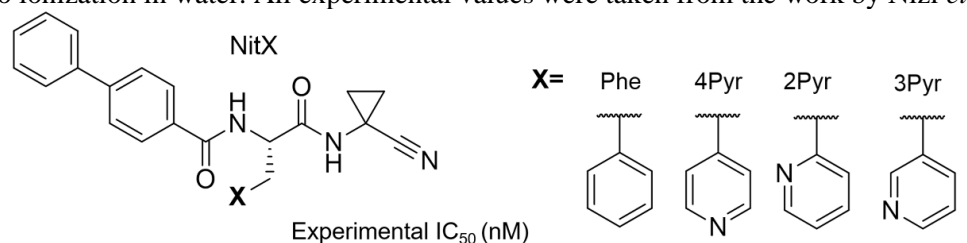


Source: Prepared by the author.

The currently known inhibitors of FP-2 can be classified in four scaffolds: *i*) suramin and derivatives, *ii*) heme and derivatives, *iii*) *E*-chalcones and *iv*) methacycline (Fig. 1.6).<sup>34-36, 38</sup> Heme and suramin are able to modulate the enzyme through an excess-substrate inhibition, which involves the interaction of a substrate molecule with a secondary binding site.<sup>34, 35</sup> The two *E*-chalcone derivatives termed Cpd48 and Cpd66 were reported to trigger a classical and mixed non-competitive inhibition against FP-2, respectively.<sup>36</sup> Cpd66 failed to protect from hydrolysis a peptide associated to the FP-2 orthosteric site, as determined by comparing the peptide mass fingerprints generated through trypsin digestion of the free enzyme and when bound to the inhibitor. However, the compound decreased in a concentration-dependent manner the generation of a tryptic peptide unrelated to the orthosteric binding site and comprising residues from N204 to R213 (loop<sub>204-213</sub>, Fig. 1.7). These results were interpreted as a supporting evidence of the non-competitive inhibition mechanism of the compound.<sup>36</sup> A valuable clue to locate the FP-2 allosteric

pocket that binds Cpd66 emerged from the previous experiment, which can be further exploited to propose a novel site for the modulation of the enzyme's catalytic activity. On the other hand, Cpd48 was co-crystallized with FP-2 and the solved structure indicates that it binds to a region comprising the prime subsites of the enzyme, which seems to be consistent with the mixed inhibition mechanism.<sup>39</sup> These findings reinforce the suitability of exploring the allosteric modulation of FP-2 in order to design novel antimalarials.

**Figure 1.8. Chemical structures and experimental  $IC_{50}$  values of the studied compounds against FPs and hCats.** Compounds marked with asterisks were tested as racemic mixtures in the inhibition assays instead of pure *S* enantiomers. Therefore, the actual  $IC_{50}$  values for these compounds are half of those reported by Nizi *et al.*, as the *R* enantiomers are inactive. N.d. stands for non-determined values. For all compounds, except for NitPhe, the values shown in the table correspond to apparent  $IC_{50}$ 's, since they undergo ionization in water. All experimental values were taken from the work by Nizi *et al.*<sup>40</sup>



Compounds	Experimental $IC_{50}$ (nM)					
	FP-2	FP-3	hCatB	hCatK	hCatL	hCatS
Nit2Pyr	>5000	n.d.	>5000	3828	>5000	>5000
Nit4Pyr	>5000	n.d.	>5000	867	755	710
Nit3Pyr	23	117	2751	202	1591	382
NitPhe	667	n.d.	2210	213	635	283
Nit6OMe3Pyr*	89	n.d.	2040	>2500	1315	98
Nit6Cl3Pyr*	115	n.d.	>2500	>2500	>2500	>2500

Source: Prepared by the author.

Despite the promising results that can be expected from allosteric compounds, their inhibitory activity is relatively modest if compared to that of orthosteric inhibitors. Instead, recent literature has drawn the attention to reversible covalent inhibitors of these enzymes, i.e., small molecules forming reversible covalent bonds with the catalytic Cys, as a good balance between affinity and selectivity can be reached by fine-tuning non-covalent interactions with the target and warhead reactivity.<sup>19</sup> Some studies have addressed this issue and have reported promising reversible covalent inhibitors of FP-2.<sup>40-43</sup> In this regard, a work by Nizi *et al.* is particularly relevant, as it demonstrates that it is possible to achieve selectivity against human cysteine cathepsins B, K, L and S (hCatB, hCatK, hCatL and hCatS, respectively) by focusing on the P2 position of peptidomimetic nitriles, i.e., peptide analogs bearing the cyano ( $-C\equiv N$ ) warhead.<sup>40</sup> Interestingly, the authors reported noticeable changes in the activity and selectivity profiles of

isomeric compounds with pyridine moieties at P2, in which the aromatic N atom ( $N_{\text{pyr}}$ ) lies at different positions (Fig. 1.8).

Among the compounds with different P2 substituents tested by Nizi *et al.*, it was Nit3Pyr (*Nit* stands for the nitrile core structure and *3Pyr*, for the P2-pyridine with the  $N_{\text{pyr}}$  atom at position 3) the one showing the highest affinity for FP-2 ( $IC_{50}=23$  nM) and selectivity against hCats (9 to 120-fold more active).<sup>40</sup> On the other hand, isomers Nit2Pyr and Nit4Pyr displayed no inhibitory activity against FP-2 (Fig. 1.8) up to 5  $\mu\text{M}$ ; whereas other Nit3Pyr derivatives, e.g., Nit6Cl3Pyr and Nit6OMe3Pyr, though still active, did not improve the affinity and selectivity of the parent compound (Fig. 1.8). Moreover, Nit3Pyr inhibits FP-3 ( $IC_{50}=117$  nM) and outperformed the inhibition against FP-2 of compounds with structurally-similar yet more hydrophobic P2 moieties, such as NitPhe ( $IC_{50}=667$  nM, Fig. 1.8).<sup>40</sup> Compound Nit3Pyr was further redesigned at P3 position, which led to better affinity and selectivity for FP-2, micromolar inhibition of *P. falciparum* growth *in vitro* and non-detectable cytotoxicity against human cell lines.<sup>40</sup> Despite these promising findings, currently there is no detailed structural knowledge on the complexes formed by the nitriles and proteases mentioned above. This lack of information precludes the rational optimization of P2-pyridine moieties and the structure-based design of novel inhibitors mimicking the Nit3Pyr properties.

On the basis of all the previous information, it becomes clear that the search for FP-2 inhibitors constitutes an active and relevant field. In spite of the current interest in this enzyme, there are some aspects requiring further study to foster the discovery of more selective FP-2 inhibitors. Therefore, in this work we intend to achieve the following general objective:

*To propose new inhibitors, druggable allosteric sites and molecular determinants for selective orthosteric inhibition of FP-2.*

To accomplish this objective, we will conduct the specific objectives shown below:

1. To identify novel competitive inhibitors of FP-2 through a combination of SBVSs and rescoring steps by taking into account the potential interaction with human off-targets, and to assess their inhibitory activity *in vitro* against FP-2, *P. falciparum* cultures, hCatK and HeLa cell-line.
2. To evaluate the suitability of site 6 of FP-2 as a druggable allosteric site by identifying ligands targeting this site through a combination of SBVSs and rescoring steps, and the subsequent determination of their inhibitory activity *in vitro* against FP-2 and their inhibition mechanism.

3. To predict the occurrence of transient allosteric cavities in FP-2 on the basis of experimental information related to the non-competitive inhibitor Cpd66 and the performance of computational analyses to determine the compound's binding mode and the inhibition mechanism at molecular level.
4. To identify the molecular determinants for the selective inhibition against FP-2 of nitriles containing 3-pyridine derivatives at position P2 through MD simulations and free energy calculations in order to enable the discovery of more selective FP-2 inhibitors.

The methodologies and experimental approaches employed here to carry out the previous specific objectives will be presented in the next chapter. Objectives 1 and 2 will be developed in Chapter 3, where four FP-2 inhibitors, two of them discovered through SVBSs against the active site, and the other two, against site 6, are presented. Chapters 4 and 5 show the results of the prediction of a novel allosteric site of FP-2 based on the experimental information related to Cpd66 and the role of water molecules in the selectivity for FP-2 of nitriles containing 3-pyridine derivatives at position P2, respectively. The main conclusions of this work are presented in Chapter 6, and four appendices (from A to D) provide supporting information to the methods and results.



## 6 CONCLUDING REMARKS

In this work we have explored different *in silico* approaches aiming at the identification of novel FP-2 inhibitors with improved selectivity. Two promising compounds, HTS07940 and HTS08262, were identified through SBVSs directed towards the active sites of FP-2, FP-3 and hCatK and subsequent experimental validation. The compounds display inhibitory activity against FP-2 in the  $10^{-5}$ - $10^{-6}$  M range and no inhibition of hCatK was detected. The higher selectivity for FP-2 was attributed to differences in the residue composition at the bottom of the S2 subsite among the analyzed cysteine proteases. In addition, HTS07940 and HTS08262 possess micromolar inhibition of *P. falciparum* growth *in vitro* and suitable selectivity indices when tested against HeLa cells. Both compounds belong to a new scaffold of FP-2 inhibitor, which increases the chemical repertoire of antimalarial drug candidates. We also probed the potential of site 6 of FP-2 as a druggable allosteric site through SBVS. Two compounds, ZINC03225317 and ZINC72290660, were identified as non-competitive FP-2 inhibitors after the experimental validation. Despite their weak inhibitory activity against FP-2,  $K_i$  values within the  $10^{-4}$ - $10^{-3}$  M range, our results show the suitability of site 6 as a druggable cavity in FP-2.

Moreover, the search for other potential allosteric cavities of FP-2 was expanded by predicting the binding mode of a reported non-competitive inhibitor, Cpd66, with available experimental information on the likely location of its binding site. The formation of a transient pocket at the site 3 region of FP-2, which remains mostly occluded by K34 side-chain, was revealed. The predicted binding mode of Cpd66 within the identified pocket fulfills all the experimental findings, thus reinforcing the potential of site 3 as an allosteric pocket. In accordance with the established classical non-competitive mechanism of Cpd66, the absence of conformational changes at the active site upon the compound binding was corroborated *in silico*. It was shown that a combination of subtle structural aspects, e.g., variations in loop motions, community and signaling pathways rearrangements, and  $pK_a$  shifts, constitute the likely molecular fingerprint of an impaired catalytic function of FP-2 when bound to Cpd66.

Finally, we conducted a computational study to decipher the bases of the selectivity for FP-2 of nitriles containing Pyr derivatives at P2. Our results revealed that water bridges involving residues I85 and D234 of FP-2, and the deprotonated nitrogen of the 3Pyr moiety at P2, which are either less prevalent or nonexistent in the analog complexes involving hCats, explain the SAR data.



The presence of water molecules in the crystal structures of the studied enzymes close to the bridging water positions reinforces the likelihood of such interactions occurring. The presence of the nitrogen atom in positions 2 and 4 of the pyridine ring, also precludes the formation of the stabilizing water bridges within the S2 subsite of FP-2. Our results show that selective FP-2 inhibitors can be designed by promoting the formation of the above-mentioned water bridge and/or by introducing substituents that displace the bridging water.

## REFERENCES

- (1) Sachs, J.; Malaney, P., The Economic and Social Burden of Malaria. . *Nature* **2002**, 415, 680–685.
- (2) World Malaria Report 2017 <http://www.who.int/malaria/publications/world-malaria-report-2017/report/en/>.
- (3) Teixeira, C.; Gomes, J. R.; Gomes, P., Falcipains, *Plasmodium falciparum* Cysteine Proteases as Key Drug Targets against Malaria. *Curr Med Chem* **2011**, 18, 1555-1572.
- (4) Rosenthal, P. J., Falcipains and Other Cysteine Proteases of Malaria Parasites. *Adv Exp Med Biol* **2011**, 712, 30-48.
- (5) Rowe, J. A.; Claessens, A.; Corrigan, R. A.; Arman, M., Adhesion of *Plasmodium falciparum*-Infected Erythrocytes to Human Cells: Molecular Mechanisms and Therapeutic Implications. *Expert Rev Mol Med* **2009**, 11, e16.
- (6) Zheng, J.; Pan, H.; Gu, Y.; Zuo, X.; Ran, N.; Yuan, Y.; Zhang, C.; Wang, F., Prospects for Malaria Vaccines: Pre-Erythrocytic Stages, Blood Stages, and Transmission-Blocking Stages. *Biomed Res Int* **2019**, 2019, 9751471.
- (7) Bekono, B. D.; Ntie-Kang, F.; Owono Owono, L. C.; Megnassan, E., Targeting Cysteine Proteases from *Plasmodium falciparum*: A General Overview, Rational Drug Design and Computational Approaches for Drug Discovery. *Curr Drug Targets* **2018**, 501-526.
- (8) Ettari, R.; Bova, F.; Zappala, M.; Grasso, S.; Micale, N., Falcipain-2 Inhibitors. *Med Res Rev* **2010**, 30, 136-167.
- (9) Shenai, B. R.; Sijwali, P. S.; Singh, A.; Rosenthal, P. J., Characterization of Native and Recombinant Falcipain-2, a Principal Trophozoite Cysteine Protease and Essential Hemoglobinase of *Plasmodium falciparum*. *J Biol Chem* **2000**, 275, 29000-29010.
- (10) Sijwali, P. S.; Shenai, B. R.; Gut, J.; Singh, A.; Rosenthal, P. J., Expression and Characterization of the *Plasmodium falciparum* Haemoglobinase Falcipain-3. *Biochem J* **2001**, 360, 481-489.
- (11) Roy, K. K., Targeting the Active Sites of Malarial Proteases for Antimalarial Drug Discovery: Approaches, Progress and Challenges. *Int J Antimicrob Agents* **2017**, 50, 287-302.
- (12) Sijwali, P. S.; Koo, J.; Singh, N.; Rosenthal, P. J., Gene Disruptions Demonstrate Independent Roles for the Four Falcipain Cysteine Proteases of *Plasmodium falciparum*. *Mol Biochem Parasitol* **2006**, 150, 96-106.
- (13) Kerr, I. D.; Lee, J. H.; Pandey, K. C.; Harrison, A.; Sajid, M.; Rosenthal, P. J.; Brinen, L. S., Structures of Falcipain-2 and Falcipain-3 Bound to Small Molecule Inhibitors: Implications for Substrate Specificity. *J Med Chem* **2009**, 52, 852-857.
- (14) Pandey, K. C.; Wang, S. X.; Sijwali, P. S.; Lau, A. L.; McKerrow, J. H.; Rosenthal, P. J., The *Plasmodium falciparum* Cysteine Protease Falcipain-2 Captures Its Substrate, Hemoglobin, Via a Unique Motif. *Proc Natl Acad Sci U S A* **2005**, 102, 9138-9143.

- (15) Sijwali, P. S.; Shenai, B. R.; Rosenthal, P. J., Folding of the *Plasmodium falciparum* Cysteine Protease Falcipain-2 Is Mediated by a Chaperone-Like Peptide and Not the Prodomain. *J Biol Chem* **2002**, *277*, 14910-14915.
- (16) Cotrin, S. S.; Gouvea, I. E.; Melo, P. M.; Bagnaresi, P.; Assis, D. M.; Araujo, M. S.; Juliano, M. A.; Gazarini, M. L.; Rosenthal, P. J.; Juliano, L.; Carmona, A. K., Substrate Specificity Studies of the Cysteine Peptidases Falcipain-2 and Falcipain-3 from *Plasmodium falciparum* and Demonstration of Their Kininogenase Activity. *Mol Biochem Parasitol* **2013**, *187*, 111-116.
- (17) Teixeira, C.; Gomes, J. R.; Couesnon, T.; Gomes, P., Molecular Docking and 3d-Quantitative Structure Activity Relationship Analyses of Peptidyl Vinyl Sulfones: *Plasmodium falciparum* Cysteine Proteases Inhibitors. *J Comput Aided Mol Des* **2011**, *25*, 763-775.
- (18) Fernandez, L.; Bustos, R. H.; Zapata, C.; Garcia, J.; Jauregui, E.; Ashraf, G. M., Immunogenicity in Protein and Peptide Based-Therapeutics: An Overview. *Curr Protein Pept Sci* **2018**, *19*, 958-971.
- (19) Cianni, L.; Feldmann, C. W.; Gilberg, E.; Gutschow, M.; Juliano, L.; Leitao, A.; Bajorath, J.; Montanari, C. A., Can Cysteine Protease Cross-Class Inhibitors Achieve Selectivity? *J Med Chem* **2019**, 10497-10525.
- (20) Lu, S.; Li, S.; Zhang, J., Harnessing Allosterity: A Novel Approach to Drug Discovery. *Med Res Rev* **2014**, *34*, 1242-1285.
- (21) Liu, J.; Nussinov, R., Allosterity: An Overview of Its History, Concepts, Methods, and Applications. *PLoS Comput Biol* **2016**, *12*, e1004966.
- (22) Nussinov, R.; Tsai, C. J., Allosterity in Disease and in Drug Discovery. *Cell* **2013**, *153*, 293-305.
- (23) Wagner, J. R.; Lee, C. T.; Durrant, J. D.; Malmstrom, R. D.; Feher, V. A.; Amaro, R. E., Emerging Computational Methods for the Rational Discovery of Allosteric Drugs. *Chem Rev* **2016**, *116*, 6370-6390.
- (24) Li, Z.; Kienetz, M.; Cherney, M. M.; James, M. N.; Bromme, D., The Crystal and Molecular Structures of a Cathepsin K:Chondroitin Sulfate Complex. *J Mol Biol* **2008**, *383*, 78-91.
- (25) Novinec, M.; Korenc, M.; Caflich, A.; Ranganathan, R.; Lenarcic, B.; Baici, A., A Novel Allosteric Mechanism in the Cysteine Peptidase Cathepsin K Discovered by Computational Methods. *Nat Commun* **2014**, *5*, 3287.
- (26) Novinec, M.; Lenarcic, B.; Baici, A., Probing the Activity Modification Space of the Cysteine Peptidase Cathepsin K with Novel Allosteric Modifiers. *PLoS One* **2014**, *9*, e106642.
- (27) Novinec, M.; Rebernik, M.; Lenarcic, B., An Allosteric Site Enables Fine-Tuning of Cathepsin K by Diverse Effectors. *FEBS Lett* **2016**, *590*, 4507-4518.
- (28) Li, Z.; Yasuda, Y.; Li, W.; Bogyo, M.; Katz, N.; Gordon, R. E.; Fields, G. B.; Bromme, D., Regulation of Collagenase Activities of Human Cathepsins by Glycosaminoglycans. *J Biol Chem* **2004**, *279*, 5470-5479.

- (29) Almeida, P. C., et al, Cathepsin B Activity Regulation. Heparin-Like Glycosaminoglycans Protect Human Cathepsin B from Alkaline pH-Induced Inactivation. *J Biol Chem* **2001**, 276, 944-951.
- (30) Judice, W. A., et al, Heparin Modulates the Endopeptidase Activity of *Leishmania mexicana* Cysteine Protease Cathepsin L-Like Rcpb2.8. *PLoS One* **2013**, 8, e80153.
- (31) Lima, A. P., et al, Heparan Sulfate Modulates Kinin Release by *Trypanosoma cruzi* through the Activity of Cruzipain. *J Biol Chem* **2002**, 277, 5875-5881.
- (32) Costa, T. F.; dos Reis, F. C.; Lima, A. P., Substrate Inhibition and Allosteric Regulation by Heparan Sulfate of *Trypanosoma brucei* Cathepsin L. *Biochim Biophys Acta* **2012** 1824, 493–501.
- (33) Almeida, P. C., et al Cysteine Proteinase Activity Regulation. A Possible Role of Heparin and Heparin-Like Glycosaminoglycans. *J Biol Chem* **1999**, 274, 30433-30438.
- (34) Marques, A. F.; Esser, D.; Rosenthal, P. J.; Kassack, M. U.; Lima, L. M., Falcipain-2 Inhibition by Suramin and Suramin Analogues. *Bioorg Med Chem* **2013**, 21, 3667-3673.
- (35) Marques, A. F.; Gomes, P. S.; Oliveira, P. L.; Rosenthal, P. J.; Pascutti, P. G.; Lima, L. M., Allosteric Regulation of the *Plasmodium falciparum* Cysteine Protease Falcipain-2 by Heme. *Arch Biochem Biophys* **2015**, 573, 92-99.
- (36) Bertoldo, J. B.; Chiaradia-Delatorre, L. D.; Mascarello, A.; Leal, P. C.; Cordeiro, M. N.; Nunes, R. J.; Sarduy, E. S.; Rosenthal, P. J.; Terenzi, H., Synthetic Compounds from an in House Library as Inhibitors of Falcipain-2 from *Plasmodium falciparum*. *J Enzyme Inhib Med Chem* **2015**, 30, 299-307.
- (37) Pant, A.; Kumar, R.; Wani, N. A.; Verma, S.; Sharma, R.; Pande, V.; Saxena, A. K.; Dixit, R.; Rai, R.; Pandey, K. C., Allosteric Site Inhibitor Disrupting Auto-Processing of Malarial Cysteine Proteases. *Sci Rep* **2018**, 8, 16193.
- (38) Alberca, L. N.; Chuguransky, S. R.; Alvarez, C. L.; Talevi, A.; Salas-Sarduy, E., *In Silico* Guided Drug Repurposing: Discovery of New Competitive and Non-Competitive Inhibitors of Falcipain-2. *Front Chem* **2019**, 7, 534.
- (39) Machin, J. M.; Kantsadi, A. L.; Vakonakis, I., The Complex of *Plasmodium falciparum* Falcipain-2 Protease with an (E)-Chalcone-Based Inhibitor Highlights a Novel, Small, Molecule-Binding Site. *Malar J* **2019**, 18, 388.
- (40) Nizi, E.; Sferrazza, A.; Fabbrini, D.; Nardi, V.; Andreini, M.; Graziani, R.; Gennari, N.; Bresciani, A.; Paonessa, G.; Harper, S., Peptidomimetic Nitrile Inhibitors of Malarial Protease Falcipain-2 with High Selectivity against Human Cathepsins. *Bioorg Med Chem Lett* **2018**, 28, 1540-1544.
- (41) Verissimo, E.; Berry, N.; Gibbons, P.; Cristiano, M. L.; Rosenthal, P. J.; Gut, J.; Ward, S. A.; O'Neill, P. M., Design and Synthesis of Novel 2-Pyridone Peptidomimetic Falcipain 2/3 Inhibitors. *Bioorg Med Chem Lett* **2008**, 18, 4210-4214.
- (42) Lee, B. J.; Singh, A.; Chiang, P.; Kemp, S. J.; Goldman, E. A.; Weinhouse, M. I.; Vlasuk, G. P.; Rosenthal, P. J., Antimalarial Activities of Novel Synthetic Cysteine Protease Inhibitors. *Antimicrob Agents Chemother* **2003**, 47, 3810-3814.

- (43) Ehmke, V.; Kilchmann, F.; Heindl, C.; Cui, K.; Huang, J.; Schirmeister, T.; Diederich, F., Peptidomimetic Nitriles as Selective Inhibitors for the Malarial Cysteine Protease Falcipain-2. *MedChemComm* **2011**, 2, 800-804.
- (44) Webb, B.; Sali, A., Comparative Protein Structure Modeling Using Modeller. *Curr Protoc Bioinformatics* **2016**, 56 1-56 37.
- (45) Dolinsky, T. J.; Czodrowski, P.; Li, H.; Nielsen, J. E.; Jensen, J. H.; Klebe, G.; Baker, N. A., PDB2PQR: Expanding and Upgrading Automated Preparation of Biomolecular Structures for Molecular Simulations. *Nucleic Acids Res* **2007**, 35, W522-525.
- (46) Marti-Renom, M. A.; Stuart, A. C.; Fiser, A.; Sanchez, R.; Melo, F.; Sali, A., Comparative Protein Structure Modeling of Genes and Genomes. *Annu Rev Biophys Biomol Struct* **2000**, 29, 291-325.
- (47) Sali, A.; Blundell, T. L., Comparative Protein Modelling by Satisfaction of Spatial Restraints. *J Mol Biol* **1993**, 234, 779-815.
- (48) Rognan, D., Docking Methods for Virtual Screening: Principles and Recent Advances. In *Virtual Screening*. Sotriffer C., Ed.; WILEY-VCH Verlag GmbH & Co. KGaA: Weinheim, 2011; Chapter 6, pp 153-176.
- (49) Trott, O.; Olson, A. J., Autodock Vina: Improving the Speed and Accuracy of Docking with a New Scoring Function, Efficient Optimization, and Multithreading. *J Comput Chem* **2010**, 31, 455-461.
- (50) Hernandez-Gonzalez, J. E.; Salas-Sarduy, E.; Hernandez Ramirez, L. F.; Pascual, M. J.; Alvarez, D. E.; Pabon, A.; Leite, V. B. P.; Pascutti, P. G.; Valiente, P. A., Identification of (4-(9H-Fluoren-9-yl) Piperazin-1-yl) Methanone Derivatives as Falcipain 2 Inhibitors Active against *Plasmodium falciparum* Cultures. *Biochim Biophys Acta Gen Subj* **2018**, 1862, 2911-2923.
- (51) Morris, G. M.; Huey, R.; Lindstrom, W.; Sanner, M. F.; Belew, R. K.; Goodsell, D. S.; Olson, A. J., Autodock4 and Autodocktools4: Automated Docking with Selective Receptor Flexibility. *J Comput Chem* **2009**, 30, 2785-2791.
- (52) Hernandez Gonzalez, J. E.; Hernandez Alvarez, L.; Pascutti, P. G.; Valiente, P. A., Predicting Binding Modes of Reversible Peptide-Based Inhibitors of Falcipain-2 Consistent with Structure-Activity Relationships. *Proteins* **2017**, 85, 1666-1683.
- (53) Hernandez Alvarez, L.; Barreto Gomes, D. E.; Hernandez Gonzalez, J. E.; Pascutti, P. G., Dissecting a Novel Allosteric Mechanism of Cruzain: A Computer-Aided Approach. *PLoS One* **2019**, 14, e0211227.
- (54) Nguyen, H.; Roe, D. R.; Simmerling, C., Improved Generalized Born Solvent Model Parameters for Protein Simulations. *J Chem Theory Comput* **2013**, 9, 2020-2034.
- (55) Case, D. A.; Babin, V.; Berryman, J. T.; Betz, R. M.; Cai, Q.; Cerutti, D. S.; T E Cheatham, I.; Darden, T. A.; Duke, R. E.; Gohlke, H.; Goetz, A. W.; Gusarov, S.; Homeyer, N.; Janowski, P.; Kaus, J.; Kolossváry, I.; Kovalenko, A.; Lee, T.; LeGrand, S.; Luchko, T.; Luo, R.; Madej, B.; Merz, K. M.; Paesani, F.; Roe, D. R.; Roitberg, A.; C Sagui; Salomon-Ferrer, R.; Seabra, G.;

Simmerling, C. L.; Smith, W.; Swails, J.; Walker, R. C.; Wang, J.; Wolf, R. M.; Wu, X.; Kollman, P. A. *Amber14* University of California, San Francisco, 2014.

(56) Frisch, M. J.; Trucks, G. W.; Schlegel, H. B.; Scuseria, G. E.; Robb, M. A.; Cheeseman, J. R.; Scalmani, G.; Barone, V.; Mennucci, B.; Petersson, G. A.; Nakatsuji, H.; Caricato, M.; Li, X.; Hratchian, H. P.; Izmaylov, A. F.; Bloino, J.; Zheng, G.; Sonnenberg, J. L.; Hada, M.; Ehara, M.; Toyota, K.; Fukuda, R.; Hasegawa, J.; Ishida, M.; Nakajima, T.; Honda, Y.; Kitao, O.; Nakai, H.; Vreven, T.; Montgomery Jr., J. A.; Peralta, J. E.; Ogliaro, F.; Bearpark, M. J.; Heyd, J.; Brothers, E. N.; Kudin, K. N.; Staroverov, V. N.; Kobayashi, R.; Normand, J.; Raghavachari, K.; Rendell, A. P.; Burant, J. C.; Iyengar, S. S.; Tomasi, J.; Cossi, M.; Rega, N.; Millam, N. J.; Klene, M.; Knox, J. E.; Cross, J. B.; Bakken, V.; Adamo, C.; Jaramillo, J.; Gomperts, R.; Stratmann, R. E.; Yazyev, O.; Austin, A. J.; Cammi, R.; Pomelli, C.; Ochterski, J. W.; Martin, R. L.; Morokuma, K.; Zakrzewski, V. G.; Voth, G. A.; Salvador, P.; Dannenberg, J. J.; Dapprich, S.; Daniels, A. D.; Farkas, Ö.; Foresman, J. B.; Ortiz, J. V.; Cioslowski, J.; Fox, D. J. *Gaussian 09*, Gaussian, Inc.: Wallingford, CT, USA, 2009.

(57) Molecular Operating Environment (MOE), 2013.08; Chemical Computing Group Inc., 1010 Sherbooke St. West, Suite #910, Montreal, QC, Canada, H3A 2R7, 2016.

(58) Hernandez Gonzalez, J. E.; Hernandez Alvarez, L.; Pascutti, P. G.; Leite, V. B. P., Prediction of Noncompetitive Inhibitor Binding Mode Reveals Promising Site for Allosteric Modulation of Falcipain-2. *J Phys Chem B* **2019**, 123, 7327-7342.

(59) Rastelli, G.; Del Rio, A.; Degliesposti, G.; Sgobba, M., Fast and Accurate Predictions of Binding Free Energies Using MM-PBSA and MM-GBSA. *J Comput Chem* **2010**, 31, 797-810.

(60) Hou, T.; Wang, J.; Li, Y.; Wang, W., Assessing the Performance of the Molecular Mechanics/Poisson Boltzmann Surface Area and Molecular Mechanics/Generalized Born Surface Area Methods. II. The Accuracy of Ranking Poses Generated from Docking. *J Comput Chem* **2011**, 32, 866-877.

(61) Hanwell, M. D.; Curtis, D. E.; Lonie, D. C.; Vandermeersch, T.; Zurek, E.; Hutchison, G. R., Avogadro: An Advanced Semantic Chemical Editor, Visualization, and Analysis Platform. *J Cheminform* **2012**, 4, 17.

(62) Case, D. A.; Betz, R. M.; Cerutti, D. S.; Cheatham III, T. E.; Darden, T. A.; Duke, R. E.; Giese, T. J.; Gohlke, H.; Goetz, A. W.; Homeyer, N.; Izadi, S.; Janowski, P.; Kaus, J.; Kovalenko, A.; Lee, T. S.; LeGrand, S.; Li, P.; Lin, C.; Luchko, T.; Luo, R.; Madej, B.; Mermelstein, D.; Merz, K. M.; Monard, G.; Nguyen, H.; Nguyen, H. T.; Omelyan, I.; Onufriev, A.; Roe, D. R.; Roitberg, A.; Sagui, C.; Simmerling, C. L.; Botello-Smith, W. M.; Swails, J.; Walker, R. C.; Wang, J.; Wolf, R. M.; Wu, X.; Xiao, L.; Kollman, P. A. *Amber 2016*, University of California, San Francisco, 2016.

(63) Case, D. A.; Ben-Shalom, I. Y.; Brozell, S. R.; Cerutti, D. S.; Cheatham III, T. E.; Cruzeiro, V. W. D.; Darden, T. A.; Duke, R. E.; Ghoreishi, D.; Gilson, M. K.; Gohlke, H.; Goetz, A. W.; Greene, D.; Harris, R.; Homeyer, N.; Izadi, S.; Kovalenko, A.; Kurtzman, T.; Lee, T. S.; LeGrand, S.; Li, P.; Lin, C.; Liu, J.; Luchko, T.; Luo, R.; Mermelstein, D. J.; Merz, K. M.; Miao, Y.; Monard, G.; Nguyen, C.; Nguyen, H.; Omelyan, I.; Onufriev, A.; Pan, F.; Qi, R.; Roe, D. R.; Roitberg, A.; Sagui, C.; Schott-Verdugo, S.; Shen, J.; Simmerling, C. L.; Smith, J.; Salomon-Ferrer, R.; Swails,

J.; Walker, R. C.; Wang, J.; Wei, H.; Wolf, R. M.; Wu, X.; Xiao, L.; York, D. M.; Kollman, P. A. *Amber 2018*, University of California, San Francisco, 2018.

(64) Wang, J.; Wolf, R. M.; Caldwell, J. W.; Kollman, P. A.; Case, D. A., Development and Testing of a General Amber Force Field. *J Comput Chem* **2004**, *25*, 1157-1174.

(65) Norberg, J.; Nilsson, L., Advances in Biomolecular Simulations: Methodology and Recent Applications. *Q. Rev. Biophys.* **2003**, *36*, 257-306.

(66) MacKerell, A. D. Atomistic Models and Force Fields. In *Computational Biochemistry and Biophysics*, Becker, O. M.; MacKerell, A. D.; Roux, B.; Watanabe, M., Eds.; Marcel Dekker, Inc.: New York, NY, 2001; Chapter 2, pp 7-38.

(67) Hug, S., Classical Molecular Dynamics in a Nutshell. *Methods Mol Biol* **2013**, *924*, 127-152.

(68) Lindahl, E. R. Molecular Dynamics Simulations. In *Methods in Molecular Biology (Methods and Protocols)*, Kukol, A., Ed.; Humana Press: New York, NY, 2015; Vol. 1215, pp 3-26.

(69) Maier, J. A.; Martinez, C.; Kasavajhala, K.; Wickstrom, L.; Hauser, K. E.; Simmerling, C., ff14SB: Improving the Accuracy of Protein Side Chain and Backbone Parameters from ff99SB. *J Chem Theory Comput* **2015**, *11*, 3696-3713.

(70) Reif, M. M.; Hunenberger, P. H.; Oostenbrink, C., New Interaction Parameters for Charged Amino Acid Side Chains in the Gromos Force Field. *J Chem Theory Comput* **2012**, *8*, 3705-3723.

(71) Abraham, M. J.; Murtola, T.; Schulz, R.; Páll, S.; Smith, J. C.; Hess, B.; Lindahl, E., Gromacs: High Performance Molecular Simulations through Multi-Level Parallelism from Laptops to Supercomputers. *SoftwareX* **2015**, *1*, 19-25.

(72) Hess, B.; Bekker, H.; Berendsen, H. J.; Fraaije, J. G., Lincs: A Linear Constraint Solver for Molecular Simulations. *J Comput Chem* **1997**, *18*, 1463-1472.

(73) Berendsen, H. J. C.; Postma, J. P. M.; van Gunsteren, W. F.; Di Nola, A.; Haak, J. R., Molecular Dynamics with Coupling to an External Bath. *J Chem Phys* **1984**, *81*, 3684-3690.

(74) Bussi, G.; Donadio, D.; Parrinello, M., Canonical Sampling through Velocity Rescaling. *J Chem Phys* **2007**, *126*, 014101.

(75) Parrinello, M.; Rahman, A., Polymorphic Transitions in Single Crystals: A New Molecular Dynamics Method. *J Appl Phys* **1981**, *52*, 7182-7190.

(76) Hamelberg, D.; Mongan, J.; McCammon, J. A., Accelerated Molecular Dynamics: A Promising and Efficient Simulation Method for Biomolecules. *J. Chem. Phys.* **2004**, *120*, 11919-11929.

(77) Wereszczynski, J.; McCammon, J. A., Accelerated Molecular Dynamics in Computational Drug Design. *Methods Mol Biol* **2012**, *819*, 515-524.

(78) Swails, J. M.; York, D. M.; Roitberg, A. E., Constant pH Replica Exchange Molecular Dynamics in Explicit Solvent Using Discrete Protonation States: Implementation, Testing, and Validation. *J Chem Theory Comput* **2014**, *10*, 1341-1352.

- (79) Socher, E.; Sticht, H., Mimicking Titration Experiments with Md Simulations: A Protocol for the Investigation of pH-Dependent Effects on Proteins. *Sci Rep* **2016**, 6, 22523.
- (80) Mathematica, Version 7.0; Wolfram Research. Inc: Champaign, Illinois, 2008.
- (81) Hayes, J. M.; Archontis, G. MM-GB(PB)SA Calculations of Protein-Ligand Binding Free Energies. In *Molecular Dynamics – Studies of Synthetic and Biological Macromolecules*, Wang, L., Ed.; InTech: Rijeka, Croatia, 2012; Chapter 9, pp 171-190.
- (82) Still, W. C.; Tempczyk, A.; Hawley, R. C.; Hendrickson, T., Semianalytical Treatment of Solvation for Molecular Mechanics and Dynamics. *J. Am. Chem. Soc.* **1990**, 112, 6127–6129.
- (83) Miller, B. R., 3rd; McGee, T. D., Jr.; Swails, J. M.; Homeyer, N.; Gohlke, H.; Roitberg, A. E., MMPBSA.py: An Efficient Program for End-State Free Energy Calculations. *J Chem Theory Comput* **2012**, 8, 3314-3321.
- (84) Maffucci, I.; Contini, A., Improved Computation of Protein-Protein Relative Binding Energies with the Nwat-MMGBSA Method. *J Chem Inf Model* **2016**, 56, 1692-1704.
- (85) Maffucci, I.; Hu, X.; Fumagalli, V.; Contini, A., An Efficient Implementation of the Nwat-MMGBSA Method to Rescore Docking Results in Medium-Throughput Virtual Screenings. *Front Chem* **2018**, 6, 43.
- (86) Martins, S. A.; Perez, M. A.; Moreira, I. S.; Sousa, S. F.; Ramos, M. J.; Fernandes, P. A., Computational Alanine Scanning Mutagenesis: MM-PBSA vs TI. *J Chem Theory Comput* **2013**, 9, 1311-1319.
- (87) Kuhn, B.; Tichy, M.; Wang, L.; Robinson, S.; Martin, R. E.; Kuglstatter, A.; Benz, J.; Giroud, M.; Schirmeister, T.; Abel, R.; Diederich, F.; Hert, J., Prospective Evaluation of Free Energy Calculations for the Prioritization of Cathepsin L Inhibitors. *J Med Chem* **2017**, 60, 2485-2497.
- (88) Gapsys, V.; Michielssens, S.; Peters, J. H.; de Groot, B. L.; Leonov, H., Calculation of Binding Free Energies. *Methods Mol Biol* **2015**, 1215, 173-209.
- (89) Chen, W.; Deng, Y.; Russell, E.; Wu, Y.; Abel, R.; Wang, L., Accurate Calculation of Relative Binding Free Energies between Ligands with Different Net Charges. *J Chem Theory Comput* **2018**, 14, 6346-6358.
- (90) Bhati, A. P.; Wan, S.; Wright, D. W.; Coveney, P. V., Rapid, Accurate, Precise, and Reliable Relative Free Energy Prediction Using Ensemble Based Thermodynamic Integration. *J Chem Theory Comput* **2017**, 13, 210-222.
- (91) Graf, M. M.; Maurer, M.; Oostenbrink, C., Free-Energy Calculations of Residue Mutations in a Tripeptide Using Various Methods to Overcome Inefficient Sampling. *J Comput Chem* **2016**, 37, 2597-2605.
- (92) Kästner, J., Umbrella Sampling. *Wiley Interdiscip. Rev. Comput. Mol. Sci.* **2011**, 1, 932-942.
- (93) Hub, J. S.; De Groot, B. L.; Van Der Spoel, D., g\_wham—A Free Weighted Histogram Analysis Implementation Including Robust Error and Autocorrelation Estimates. *J Chem Theory Comput* **2010**, 6, 3713-3720.



- (94) Doudou, S.; Burton, N. A.; Henchman, R. H., Standard Free Energy of Binding from a One-Dimensional Potential of Mean Force. *J Chem Theory Comput* **2009**, *5*, 909-918.
- (95) Lindorff-Larsen, K.; Piana, S.; Palmo, K.; Maragakis, P.; Klepeis, J. L.; Dror, R. O.; Shaw, D. E., Improved Side-Chain Torsion Potentials for the Amber ff99SB Protein Force Field. *Proteins* **2010**, *78*, 1950-1958.
- (96) Wagner, J. R.; Sorensen, J.; Hensley, N.; Wong, C.; Zhu, C.; Perison, T.; Amaro, R. E., POVME 3.0: Software for Mapping Binding Pocket Flexibility. *J Chem Theory Comput* **2017**, *13*, 4584-4592.
- (97) Bowerman, S.; Wereszczynski, J., Detecting Allosteric Networks Using Molecular Dynamics Simulation. *Methods Enzymol* **2016**, *578*, 429-447.
- (98) Sethi, A.; Eargle, J.; Black, A. A.; Luthey-Schulten, Z., Dynamical Networks in Trna:Protein Complexes. *Proc Natl Acad Sci U S A* **2009**, *106*, 6620-6625.
- (99) Girvan, M.; Newman, M. E., Community Structure in Social and Biological Networks. *Proc Natl Acad Sci U S A* **2002**, *99*, 7821-7826.
- (100) Yao, X. Q.; Malik, R. U.; Griggs, N. W.; Skjaerven, L.; Traynor, J. R.; Sivaramakrishnan, S.; Grant, B. J., Dynamic Coupling and Allosteric Networks in the Alpha Subunit of Heterotrimeric G Proteins. *J Biol Chem* **2016**, *291*, 4742-4753.
- (101) Van Wart, A. T.; Durrant, J.; Votapka, L.; Amaro, R. E., Weighted Implementation of Suboptimal Paths (Wisp): An Optimized Algorithm and Tool for Dynamical Network Analysis. *J Chem Theory Comput* **2014**, *10*, 511-517.
- (102) Lange, O. F.; Grubmuller, H., Generalized Correlation for Biomolecular Dynamics. *Proteins* **2006**, *62*, 1053-1061.
- (103) Skjaerven, L.; Yao, X. Q.; Scarabelli, G.; Grant, B. J., Integrating Protein Structural Dynamics and Evolutionary Analysis with Bio3d. *BMC Bioinformatics* **2014**, *15*, 399.
- (104) Amadei, A.; Linssen, A. B. M.; Berendsen, H. J. C., Essential Dynamics of Proteins *Proteins* **1993**, *17*, 412-425.
- (105) DeLano, W. L. *Pymol*, 2.1.0; DeLano Scientific: San Carlos, CA, 700, 2002.
- (106) Humphrey, W.; Dalke, A.; Schulten, K., Vmd: Visual Molecular Dynamics. *J Mol Graph* **1996**, *14*, 33-38, 27-38.
- (107) Lerbret, A.; Mason, P. E.; Venable, R. M.; Cesaro, A.; Saboungi, M. L.; Pastor, R. W.; Brady, J. W., Molecular Dynamics Studies of the Conformation of Sorbitol. *Carbohydr Res* **2009**, *344*, 2229-2235.
- (108) Sarduy, E. S.; Munoz, A. C.; Trejo, S. A.; de los, A. C. P. M., High-Level Expression of Falcipain-2 in Escherichia Coli by Codon Optimization and Auto-Induction. *Protein Expr Purif* **2012**, *83*, 59-69.

- (109) Linnevers, C. J.; McGrath, M. E.; Armstrong, R.; Mistry, F. R.; Barnes, M. G.; Klaus, J. L.; Palmer, J. T.; Katz, B. A.; Bromme, D., Expression of Human Cathepsin K in *Pichia Pastoris* and Preliminary Crystallographic Studies of an Inhibitor Complex. *Protein Sci* **1997**, 6, 919-921.
- (110) GraphPad Software, La Jolla California USA, [www.graphpad.com](http://www.graphpad.com).
- (111) Trager, W.; Jensen, J. B., Human Malaria Parasites in Continuous Culture. *Science* **1976**, 193, 673-675.
- (112) Pabon, A.; Ramirez, O.; Rios, A.; Lopez, E.; de Las Salas, B.; Cardona, F.; Blair, S., Antiplasmodial and Cytotoxic Activity of Raw Plant Extracts as Reported by Knowledgeable Indigenous People of the Amazon Region (Vaupes Medio in Colombia). *Planta Med* **2016**, 82, 717-722.
- (113) Bianco, A. E.; Favaloro, J. M.; Burkot, T. R.; Culvenor, J. G.; Crewther, P. E.; Brown, G. V.; Anders, R. F.; Coppel, R. L.; Kemp, D. J., A Repetitive Antigen of *Plasmodium falciparum* That Is Homologous to Heat Shock Protein 70 of *Drosophila Melanogaster*. *Proc Natl Acad Sci U S A* **1986**, 83, 8713-8717.
- (114) Pascual, M. J.; Merwaiss, F.; Leal, E.; Quintana, M. E.; Capozzo, A. V.; Cavasotto, C. N.; Bollini, M.; Alvarez, D. E., Structure-Based Drug Design for Envelope Protein E2 Uncovers a New Class of Bovine Viral Diarrhea Inhibitors That Block Virus Entry. *Antiviral Res* **2018**, 149, 179-190.
- (115) Copeland, R. A. Assay Considerations for Compound Library Screening In *Evaluation of Enzyme Inhibitors in Drug Discovery: A Guide for Medicinal Chemists and Pharmacologists*; John Wiley & Sons: 2013; Chapter 4, pp 123-168.
- (116) Selwyn, M. J., A Simple Test for Inactivation of an Enzyme During Assay. *Biochim Biophys Acta* **1965**, 105, 193-195.
- (117) In *Assay Guidance Manual*, Sittampalam, G. S.; Grossman, A.; Brimacombe, K.; Arkin, M.; Auld, D.; Austin, C. P.; Baell, J.; Bejcek, B.; Caaveiro, J. M. M.; Chung, T. D. Y.; Coussens, N. P.; Dahlin, J. L.; Devanaryan, V.; Foley, T. L.; Glicksman, M.; Hall, M. D.; Haas, J. V.; Hoare, S. R. J.; Inglese, J.; Iversen, P. W.; Kahl, S. D.; Kales, S. C.; Kirshner, S.; Lal-Nag, M.; Li, Z.; McGee, J.; McManus, O.; Riss, T.; Saradjian, P.; Trask, O. J., Jr.; Weidner, J. R.; Wildey, M. J.; Xia, M.; Xu, X., Eds.; Bethesda (MD), 2004.
- (118) Ettari, R.; Zappala, M.; Micale, N.; Grazioso, G.; Giofre, S.; Schirmeister, T.; Grasso, S., Peptidomimetics Containing a Vinyl Ketone Warhead as Falcipain-2 Inhibitors. *Eur J Med Chem* **2011**, 46, 2058-2065.
- (119) Alves, M. F.; Puzer, L.; Cotrin, S. S.; Juliano, M. A.; Juliano, L.; Bromme, D.; Carmona, A. K., S3 to S3' Subsite Specificity of Recombinant Human Cathepsin K and Development of Selective Internally Quenched Fluorescent Substrates. *Biochem J* **2003**, 373, 981-986.
- (120) Turk, V.; Stoka, V.; Vasiljeva, O.; Renko, M.; Sun, T.; Turk, B.; Turk, D., Cysteine Cathepsins: From Structure, Function and Regulation to New Frontiers. *Biochim Biophys Acta* **2012**, 1824, 68-88.

- (121) Cotrin, S. S.; Puzer, L.; de Souza Judice, W. A.; Juliano, L.; Carmona, A. K.; Juliano, M. A., Positional-Scanning Combinatorial Libraries of Fluorescence Resonance Energy Transfer Peptides to Define Substrate Specificity of Carboxydipeptidases: Assays with Human Cathepsin B. *Anal Biochem* **2004**, 335, 244-252.
- (122) Puzer, L.; Cotrin, S. S.; Alves, M. F.; Egborge, T.; Araujo, M. S.; Juliano, M. A.; Juliano, L.; Bromme, D.; Carmona, A. K., Comparative Substrate Specificity Analysis of Recombinant Human Cathepsin V and Cathepsin L. *Arch Biochem Biophys* **2004**, 430, 274-283.
- (123) Bromme, D.; Bonneau, P. R.; Lachance, P.; Storer, A. C., Engineering the S2 Subsite Specificity of Human Cathepsin S to a Cathepsin L- and Cathepsin B-Like Specificity. *J Biol Chem* **1994**, 269, 30238-30242.
- (124) Baell, J. B.; Holloway, G. A., New Substructure Filters for Removal of Pan Assay Interference Compounds (PAINS) from Screening Libraries and for Their Exclusion in Bioassays. *J Med Chem* **2010**, 53, 2719-2740.
- (125) Kuo, M. R.; Morbidoni, H. R.; Alland, D.; Sneddon, S. F.; Gourlie, B. B.; Staveski, M. M.; Leonard, M.; Gregory, J. S.; Janjigian, A. D.; Yee, C.; Musser, J. M.; Kreiswirth, B.; Iwamoto, H.; Perozzo, R.; Jacobs, W. R., Jr.; Sacchettini, J. C.; Fidock, D. A., Targeting Tuberculosis and Malaria through Inhibition of Enoyl Reductase: Compound Activity and Structural Data. *J Biol Chem* **2003**, 278, 20851-20859.
- (126) Powers, J. C.; Asgian, J. L.; Ekici, O. D.; James, K. E., Irreversible Inhibitors of Serine, Cysteine, and Threonine Proteases. *Chem Rev* **2002**, 102, 4639-4750.
- (127) Storer, A. C.; Ménard, R., Recent Insights into Cysteine Protease Specificity: Lessons for Drug Design. *Perfect Drug Discovery Des* **1996**, 6, 33-46.
- (128) Shah, F.; Mukherjee, P.; Gut, J.; Legac, J.; Rosenthal, P. J.; Tekwani, B. L.; Avery, M. A., Identification of Novel Malarial Cysteine Protease Inhibitors Using Structure-Based Virtual Screening of a Focused Cysteine Protease Inhibitor Library. *J Chem Inf Model* **2011**, 51, 852-864.
- (129) Changeux, J. P.; Edelstein, S., Conformational Selection or Induced Fit? 50 Years of Debate Resolved. *F1000 Biol Rep* **2011**, 3, 19.
- (130) Hernandez Alvarez, L.; Naranjo Feliciano, D.; Hernandez Gonzalez, J. E.; Soares, R. O.; Barreto Gomes, D. E.; Pascutti, P. G., Insights into the Interactions of Fasciola Hepatica Cathepsin L3 with a Substrate and Potential Novel Inhibitors through *In Silico* Approaches. *PLoS Negl Trop Dis* **2015**, 9, e0003759.
- (131) Durrant, J. D.; Keranen, H.; Wilson, B. A.; McCammon, J. A., Computational Identification of Uncharacterized Cruzain Binding Sites. *PLoS Negl Trop Dis* **2010**, 4, e676.
- (132) Brady, C. P.; Brinkworth, R. I.; Dalton, J. P.; Dowd, A. J.; Verity, C. K.; Brindley, P. J., Molecular Modeling and Substrate Specificity of Discrete Cruzipain-Like and Cathepsin L-Like Cysteine Proteinases of the Human Blood Fluke *Schistosoma Mansoni*. *Arch Biochem Biophys* **2000**, 380, 46-55.

- (133) Lecaille, F.; Choe, Y.; Brandt, W.; Li, Z.; Craik, C. S.; Bromme, D., Selective Inhibition of the Collagenolytic Activity of Human Cathepsin K by Altering Its S2 Subsite Specificity. *Biochemistry* **2002**, 41, 8447-8454.
- (134) Lecaille, F.; Chowdhury, S.; Purisima, E.; Bromme, D.; Lalmanach, G., The S2 Subsites of Cathepsins K and L and Their Contribution to Collagen Degradation. *Protein Sci* **2007**, 16, 662-670.
- (135) Xu, L.; Sun, H.; Li, Y.; Wang, J.; Hou, T., Assessing the Performance of MM/PBSA and MM/GBSA Methods. 3. The Impact of Force Fields and Ligand Charge Models. *J Phys Chem B* **2013**, 117, 8408-8421.
- (136) Genheden, S.; Ryde, U., The MM/PBSA and MM/GBSA Methods to Estimate Ligand-Binding Affinities. *Expert Opin Drug Discov* **2015**, 10, 449-461.
- (137) Copeland, R. A. Reversible Inhibitors. In *Enzymes: A Practical Introduction to Structure, Mechanism, and Data Analysis*; Wiley-VCH, Inc.: New York, 2000; Chapter 8, pp 266-304.
- (138) Waller, R. F.; Keeling, P. J.; Donald, R. G.; Striepen, B.; Handman, E.; Lang-Unnasch, N.; Cowman, A. F.; Besra, G. S.; Roos, D. S.; McFadden, G. I., Nuclear-Encoded Proteins Target to the Plastid in *Toxoplasma gondii* and *Plasmodium falciparum*. *Proc Natl Acad Sci U S A* **1998**, 95, 12352-12357.
- (139) Nicoll-Griffith, D. A., Use of Cysteine-Reactive Small Molecules in Drug Discovery for Trypanosomal Disease. *Expert Opin Drug Discov* **2012**, 7, 353-366.
- (140) Verespy, S., 3rd; Mehta, A. Y.; Afosah, D.; Al-Horani, R. A.; Desai, U. R., Allosteric Partial Inhibition of Monomeric Proteases. Sulfated Coumarins Induce Regulation, Not Just Inhibition, of Thrombin. *Sci Rep* **2016**, 6, 24043.
- (141) Ghisaidoobe, A. B.; Chung, S. J., Intrinsic Tryptophan Fluorescence in the Detection and Analysis of Proteins: A Focus on Forster Resonance Energy Transfer Techniques. *Int J Mol Sci* **2014**, 15, 22518-22538.
- (142) Lang, E. J.; Heyes, L. C.; Jameson, G. B.; Parker, E. J., Calculated pKa Variations Expose Dynamic Allosteric Communication Networks. *J Am Chem Soc* **2016**, 138, 2036-2045.
- (143) Bowman, G. R.; Geissler, P. L., Equilibrium Fluctuations of a Single Folded Protein Reveal a Multitude of Potential Cryptic Allosteric Sites. *Proc Natl Acad Sci U S A* **2012**, 109, 11681-11686.
- (144) Motlagh, H. N.; Wrabl, J. O.; Li, J.; Hilser, V. J., The Ensemble Nature of Allostery. *Nature* **2014**, 508, 331-339.
- (145) Tsai, C. J.; del Sol, A.; Nussinov, R., Allostery: Absence of a Change in Shape Does Not Imply That Allostery Is Not at Play. *J Mol Biol* **2008**, 378, 1-11.
- (146) Cooper, A.; Dryden, D. T., Allostery without Conformational Change. A Plausible Model. *Eur Biophys J* **1984**, 11, 103-109.
- (147) Nussinov, R.; Tsai, C. J., Allostery without a Conformational Change? Revisiting the Paradigm. *Curr Opin Struct Biol* **2015**, 30, 17-24.

- (148) Ma, W.; Tang, C.; Lai, L., Specificity of Trypsin and Chymotrypsin: Loop-Motion-Controlled Dynamic Correlation as a Determinant. *Biophys J* **2005**, 89, 1183-1193.
- (149) Eisenmesser, E. Z.; Millet, O.; Labeikovsky, W.; Korzhnev, D. M.; Wolf-Watz, M.; Bosco, D. A.; Skalicky, J. J.; Kay, L. E.; Kern, D., Intrinsic Dynamics of an Enzyme Underlies Catalysis. *Nature* **2005**, 438, 117-121.
- (150) Storer, A. C.; Menard, R., Catalytic Mechanism in Papain Family of Cysteine Peptidases. *Methods Enzymol* **1994**, 244, 486-500.
- (151) Otto, H. H.; Schirmeister, T., Cysteine Proteases and Their Inhibitors. *Chem Rev* **1997**, 97, 133-172.
- (152) Shokhen, M.; Khazanov, N.; Albeck, A., Challenging a Paradigm: Theoretical Calculations of the Protonation State of the Cys25-His159 Catalytic Diad in Free Papain. *Proteins* **2009**, 77, 916-926.
- (153) Zhai, X.; Meek, T. D., Catalytic Mechanism of Cruzain from *Trypanosoma cruzi* as Determined from Solvent Kinetic Isotope Effects of Steady-State and Pre-Steady-State Kinetics. *Biochemistry* **2018**, 57, 3176-3190.
- (154) Haynes, W. M., *Crc Handbook of Chemistry and Physics*. CRC press: 2014.
- (155) Herschlag, D.; Pinney, M. M., Hydrogen Bonds: Simple after All? *Biochemistry* **2018**, 57, 3338-3352.
- (156) Jencks, W. P., On the Attribution and Additivity of Binding Energies. *Proc Natl Acad Sci U S A* **1981**, 78, 4046-4050.
- (157) Ward, W. H.; Holdgate, G. A., Isothermal Titration Calorimetry in Drug Discovery. *Prog Med Chem* **2001**, 38, 309-376.
- (158) Song, L. F.; Lee, T. S.; Zhu, C.; York, D. M.; Merz, K. M., Jr., Using Amber18 for Relative Free Energy Calculations. *J Chem Inf Model* **2019**, 59, 3128-3135.
- (159) Xu, H.; Stern, H. A.; Berne, B. J., Can Water Polarizability Be Ignored in Hydrogen Bond Kinetics? *J Phys Chem B* **2002**, 106, 2054-2060.
- (160) Lu, J.; Hou, X.; Wang, C.; Zhang, Y., Incorporating Explicit Water Molecules and Ligand Conformation Stability in Machine-Learning Scoring Functions. *J Chem Inf Model* **2019**, 59, 4540-4549.
- (161) Huang, N.; Shoichet, B. K., Exploiting Ordered Waters in Molecular Docking. *J Med Chem* **2008**, 51, 4862-4865.
- (162) Amaro, R. E.; Li, W. W., Emerging Methods for Ensemble-Based Virtual Screening. *Curr Top Med Chem* **2010**, 10, 3-13.
- (163) Garcia-Sosa, A. T., Hydration Properties of Ligands and Drugs in Protein Binding Sites: Tightly-Bound, Bridging Water Molecules and Their Effects and Consequences on Molecular Design Strategies. *J Chem Inf Model* **2013**, 53, 1388-1405.

(164) Wang, L.; Wu, Y.; Deng, Y.; Kim, B.; Pierce, L.; Krilov, G.; Lupyan, D.; Robinson, S.; Dahlgren, M. K.; Greenwood, J.; Romero, D. L.; Masse, C.; Knight, J. L.; Steinbrecher, T.; Beuming, T.; Damm, W.; Harder, E.; Sherman, W.; Brewer, M.; Wester, R.; Murcko, M.; Frye, L.; Farid, R.; Lin, T.; Mobley, D. L.; Jorgensen, W. L.; Berne, B. J.; Friesner, R. A.; Abel, R., Accurate and Reliable Prediction of Relative Ligand Binding Potency in Prospective Drug Discovery by Way of a Modern Free-Energy Calculation Protocol and Force Field. *J Am Chem Soc* **2015**, 137, 2695-2703.

(165) Cournia, Z.; Allen, B.; Sherman, W., Relative Binding Free Energy Calculations in Drug Discovery: Recent Advances and Practical Considerations. *J Chem Inf Model* **2017**, 57, 2911-2937.

(166) Shah, F.; Gut, J.; Legac, J.; Shivakumar, D.; Sherman, W.; Rosenthal, P. J.; Avery, M. A., Computer-Aided Drug Design of Falcipain Inhibitors: Virtual Screening, Structure-Activity Relationships, Hydration Site Thermodynamics, and Reactivity Analysis. *J Chem Inf Model* **2012**, 52, 696-710.